

Florian Lackner, BSc.

Optimization of stilbene syntheses via chemo-enzymatic tandem reactions in continuous flow

MASTER'S THESIS

to achieve the university degree of

Diplom-Ingenieur

submitted to the

Graz University of Technology

Supervisors

Assoc. Prof. Dipl.-Ing. Dr.techn. Gruber-Wölfler Heidrun

Dipl.-Ing. Dr.techn. Bianca Grabner, BSc.

Katharina Hiebler, MSc. BSc.

Institute of Process and Particle Engineering

Graz, October 2020

AFFIDAVIT

I declare that I have authored this thesis independently, that I have not used other than the declared sources/resources, and that I have explicitly indicated all material which has been quoted either literally or by content from the sources used. The text document uploaded to TUGRAZonline is identical to the present master's thesis.

Date, Signature

Acknowledgement

I would like to thank the Institute of Process and Particle Engineering with the head Prof. Khinast and especially Assoc.Prof. Gruber-Wölfler and for giving me the opportunity to conduct my master thesis at the institute.

A special thanks goes to my supervisor Katharina Hiebler, who always supported me throughout my work with ideas, material and extraordinary helpful corrections of this thesis. I especially appreciate the freedom you gave me to follow my ideas during my work and keeping the English of this thesis at an acceptable level. Further thank you to Bianca Grabner, who perfectly introduced me into this topic and the world of flow chemistry.

The friendly and positive working atmosphere in this group was always a pleasure and helped me to keep a good mood even if experiments didn't work at first. Therefore, thank you to everyone in the CoSy-Pro group.

At the end, I would like to thank my family, friends and my girlfriend Victoria for your support and time. Having people in the background who are always there for you makes life and studying much easier. Perfectly written scripts, summaries and exercises for every exam helped of course too and therefore, special thanks to Simone Santner for sharing tons of documents that supported the whole chemists crew.

Abstract

The natural occurring stilbenes, resveratrol and pterostilbene, are beneficial for a plethora of biological processes in the human body and show anti-inflammation, -diabetes, -cancer and -obesity activities.

Within the framework of this master's thesis, the aim was to optimize a chemoenzymatic tandem process producing hydroxystilbene in flow and extending the product scope to resveratrol and pterostilbene. Starting from easily accessible coumaric acid, the first step of the reaction cascade was an enzymatic decarboxylation using encapsulated *BsPAD* to generate vinylphenol, which was subsequently coupled with various iodoaryl substrates via a heterogeneous palladium catalyzed Heck reaction. While the decarboxylation worked with full conversion, the Heck type coupling reaction was identified as bottleneck of the system. For this step, optimum process conditions for pH-value and K_2CO_3 concentration were evaluated in batch experiments. Optimization of the reaction temperature in flow further helped to improve the system. Compared to previous works the yield of hydroxystilbene (54.5 %) could be more than doubled in a continuous process, stable for over 300 minutes. Also, resveratrol and pterostilbene could be synthesized in flow with a yield of 32.1 % and 50.1 %, respectively.

As catalyst degradation and leaching played a major role throughout this thesis and limited the process in many perspectives, the concept of palladium swing catalysis was introduced. The active leached catalyst species was retained within the reactor zone by changing the flow direction periodically and the feasibility of this concept could be proven experimentally.

Kurzfassung

Die natürlich vorkommenden Stilbene, Resveratrol und Pterostilben, sind aufgrund ihrer entzündungshemmenden Eigenschaften sowie ihrer präventiven Wirkung gegen Diabetes, Krebs und Fettleibigkeit für zahlreiche biologische Prozesse im menschlichen Körper nützlich.

Im Zuge dieser Masterarbeit wurde ein kontinuierlicher chemo-enzymatischer Prozess zur Synthese von Hydroxystilben optimiert und zusätzlich das Produktspektrum um Resveratrol und Pterostilben erweitert. Als Ausgangssubstrat wurde Cumarsäure verwendet. Im ersten Schritt des Prozesses erfolgte eine enzymatische Decarboxylierung mithilfe von immobilisiertem *BsPAD* Enzym, welche das Zwischenprodukt Vinylphenol lieferte. Dieses wurde im darauffolgenden Schritt, der palladiumkatalysierten Heck-Kupplung, mit verschiedenen Iodoaryl-Substraten zu den jeweiligen Produkten umgesetzt. Es zeigte sich, dass die Decarboxylierung vollständigen Produktumsatz lieferte, die Heck-Kupplung jedoch den Prozess limitierte. Um diesen limitierenden Reaktionsschritt zu optimieren, wurden Batchexperimente durchgeführt und die idealen Prozessbedingungen für den pH-Wert und die K_2CO_3 Konzentration ermittelt. Weiters wurde die Reaktionstemperatur im kontinuierlichen Prozess optimiert, wodurch die Ausbeute zusätzlich verbessert werden konnte. Diese konnte so im Vergleich zu vorgehenden Arbeiten in Bezug auf Hydroxystilben mehr als verdoppelt werden (54.5 %), in einem stabilen Prozess über einen Zeitraum von 300 Minuten. Zusätzlich konnten Resveratrol und Pterostilben mit 32.1 % bzw. 50.1 % Ausbeute synthetisiert werden.

Nachdem Deaktivierung und Auslaugen des Katalysators den Syntheseprozess in vielerlei Hinsicht limitierten, wurde das Konzept der „palladium swing catalysis“ erarbeitet. Dabei wird die katalytisch aktive Spezies durch periodischen Wechsel der Flussrichtung innerhalb der Reaktionszone gehalten. Die praktische Umsetzbarkeit dieses Konzepts konnte experimentell demonstriert werden.

Contents

1	Motivation.....	1
2	Introduction.....	2
2.1	Stilbene and Derivatives.....	2
2.1.1	Resveratrol.....	2
2.1.2	Pterostilbene and 3'-Hydroxypterostilbene.....	3
2.2	Flow Chemistry.....	4
2.3	Chemo-Enzymatic Flow Set-ups.....	5
2.4	Heterogenous Heck Reactions.....	6
2.5	Coumaric Acid and Enzymatic Decarboxylation of Phenolic Acids.....	10
2.6	Enzyme Immobilization.....	12
3	Results and Discussion.....	14
3.1	Optimization of Process Conditions in Batch.....	14
3.1.1	Optimum pH-value.....	15
3.1.2	Optimum Carbonate Concentration.....	16
3.2	Heck coupling in Continuous Flow.....	17
3.2.1	Continuous Synthesis of Hydroxystilbene 4	19
3.2.2	Continuous Synthesis of Resveratrol 6	20
3.2.3	Continuous Synthesis of Pterostilbene 8	21
3.3	Tandem Flow Experiments.....	23
3.3.1	Continuous Tandem Synthesis of Hydroxystilbene 4	24
3.3.2	Continuous Tandem Synthesis of Resveratrol 6	25
3.3.3	Continuous Tandem Synthesis of Pterostilbene 8	26
3.4	Evaluation of Downstream Possibilities.....	27
3.5	Catalyst Leaching Experiments and Palladium Swing Catalysis.....	29
4	Experimental.....	34
4.1	Equipment.....	34
4.1.1	Flow Equipment.....	34
4.1.2	Batch Equipment.....	34

4.2	Analytics.....	35
4.2.1	High Performance Liquid Chromatography.....	35
4.2.2	pH-Meter	37
4.2.3	Flow-through UV-Vis Spectrometry	37
4.2.4	Thin Layer Chromatography.....	37
4.3	Batch Experiments and Synthesis.....	37
4.3.1	Deep Eutectic Solvent Preparation.....	37
4.3.2	Potassium Phosphate Buffer (KPi-Buffer) Preparation	37
4.3.3	Synthesis of Palladium Solution Combustion Catalyst $Ce_{0.2}Sn_{0.79}Pd_{0.01}O_{2.5}$	37
4.3.4	Enzyme Immobilization for the Preparation of Alginate Beads.....	38
4.3.5	General Procedure Heck Coupling Experiments	38
4.3.6	Synthesis of 5-iodobenzene-1,3-diol 5	39
4.3.7	Synthesis of 3,5-dimethoxy-1-iodobenzene 7	40
4.4	Continuous Experiments	40
4.4.1	Single Step Heck Coupling Flow Experiments.....	40
4.4.2	Chemo Enzymatic Tandem Flow Experiments	42
4.4.3	Residence Time Distribution Measurements	43
4.4.4	Leaching experiments	45
5	Conclusion and Outlook.....	46
6	Appendix	49
7	Abbreviations and Symbol Directory.....	54
8	List of Figures.....	56
9	List of Schemes.....	58
10	List of Tables.....	59
11	Bibliography.....	60

1 Motivation

Resveratrol represents one of the most studied stilbenes and the interest in this compound has extensively increased in the recent years. There is scientific evidence that resveratrol is beneficial for a plethora of biological processes in the human body, such as anti-inflammation, -diabetes, -cancer and -obesity activities.¹ Pterostilbene possesses similar useful effects but shows enhanced bioavailability due its membrane permeability.¹ As these stilbenes find application as pharmaceuticals and food supplements, a continuous high-volume industrial production is required for commercial applications to replace current production methods based on natural plants harvesting.²

In a previous work, Grabner³ and Gavric⁴ developed a chemoenzymatic tandem process to produce hydroxystilbene in flow. Starting from coumaric acid, an enzymatic decarboxylation using encapsulated *Bacillus subtilis* phenolic acid decarboxylase (*BsPAD*) gave vinylphenol, which was coupled with iodobenzene in a palladium catalyzed Heck reaction. However, the average yield of this cascade never exceeded 25 %. Therefore, the goal of this work was to optimize this system and in particular the Heck coupling part, which was identified as the bottleneck of the cascade. Especially the parameters pH-value, carbonate concentration and temperature were aimed to be investigated in more detail. Furthermore, only the resveratrol derivative hydroxystilbene has been synthesized in previous work. Therefore, the synthesis of naturally occurring compounds pterostilbene and resveratrol in continuous flow was targeted. Also, the development of a stable process over a long period should be ensured including investigation of catalyst degradation and stability.

2 Introduction

2.1 Stilbene and Derivatives

Stilbene, the core structure of the synthesized products in this thesis, was discovered by the French chemist Auguste Laurent in 1843 and could be classified as diarylethene.⁵ Two geometric isomers are known, however the *trans*-isomer is the thermodynamically favored alignment of the phenyl groups. Under UV radiation, a photochemical reaction induces a *cis-trans*-isomerization, which could further lead to the irreversible formation of phenanthrene.⁶ Likewise, light induced isomerization could be observed for derivatives of stilbene such as resveratrol, which shows this behavior at wavelengths of 350 nm and lower.^{7,8}

Stilbene itself is of little value as a chemical but it is the backbone of many important biologically active derivatives (Figure 1), which are attributed to the group of polyphenolic compounds. Many of these derivatives are naturally found in a wide variety of dietary sources and medicinal plants. Resveratrol and pterostilbene with the active metabolite 3'-hydroxypterostilbene are two of the most important and intensively studied representatives of this group and are therefore discussed in more detail in the following sections.¹

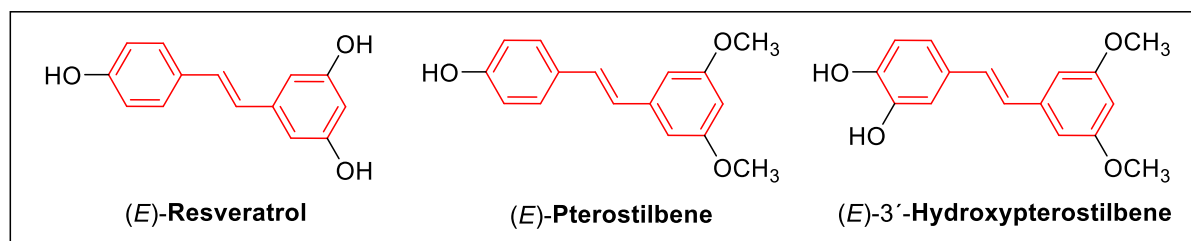


Figure 1 Structures of important biologically active stilbene derivatives (stilbene core-structure highlighted in red)

2.1.1 Resveratrol

Resveratrol was first isolated and characterized by Michio Takaoka in 1939, who extracted it from the medicinal plant roots of the white hellebore (*veratrum grandiflorum*) in Japan.⁹ As a natural polyphenolic compound, it is produced by plants to protect themselves from injury, UV irradiation and fungal attack. Human food sources of resveratrol are mainly grapes and red wine, however, it has been detected also in many other plants like peanuts, berries and pistachios. It represents one of the most studied stilbenes and the interest in this compound has extensively increased in the recent years as there is scientific evidence that resveratrol is beneficial for a plethora of biological processes in the human body. Similar to its role in plant cells, it shows a protective effect against chronic diseases, such as anti-inflammation, -diabetes, -cancer and -obesity activities.¹

The main cause for many human diseases like cancer is chronic inflammation. These inflammatory processes induce DNA mutation via oxidative or nitrosative stress and may disrupt the normal cell function.¹⁰ Mouse model experiments conducted by Cui et al. demonstrated that resveratrol could significantly suppress inflammation markers such as inducible nitric oxide synthase.¹¹ Lee et al. suggested in recent studies that resveratrol could increase the bioavailability of apigenin and therefore acts as biological enhancer. The plasma concentration of this anti-inflammatory bioactive flavonoid could be increased up to 2.39 times with a cotreatment of apigenin and resveratrol compared to simple apigenin intake.¹²

The anticancerogenic effect of resveratrol via multiple pathways has been investigated in numerous studies focusing on different kinds of cancer for example breast, prostate and colon cancer. The detailed examination of cellular cancer mechanisms showed that resveratrol affects various pathways. These include inhibition of breast cancer cell proliferation due to apoptosis, cell cycle arrest and autophagy as well as induced cytotoxic effects by reactive oxygen species to tackle colon cancer cells.¹ Further therapeutic effects of resveratrol in terms of obesity prevention could be experimentally demonstrated by using a high fat diet induced obese mice model. Chang et al. demonstrated that an administration of 1-30 mg resveratrol per kilogram bodyweight could significantly reduce the body weight gain within 10 weeks.¹³

As a consequence of the mentioned manifold therapeutic applications of (*E*)-resveratrol, a straightforward commercial production process is of high importance. At the present time it is mainly collected from natural sources like the *Polygonum* root extract. The main producing companies are located in China and depend on natural plant harvesting.² Therefore, an economically and environmentally friendly chemical or biotechnologically production is strongly desired. Kiselev reviewed different microbiological strategies and the highest rate of production could be detected with in-vitro suspension cultures that reached up to 1.3 g/L per day. However, this technology uses expensive elicitors to maintain the high production levels in plant cell cultures and are therefore limited in their commercial applicability. The best bacterial cultures only reach a ten times lower production rate compared to plant cell cultures.² In this thesis, a completely different approach using a chemoenzymatic tandem in flow is used to produce resveratrol and some analogous from low value sources.

2.1.2 Pterostilbene and 3'-Hydroxypterostilbene

Although resveratrol has been reported to possess many pharmacological effects, one issue for medical applications is its low systemic bioavailability, which reduces its potential effectivity. Instead, pterostilbene exhibits a much higher bioavailability as it shows an enhanced membrane permeability. This is based on higher lipophilicity due to two extra methoxy groups in its chemical structure (Figure 1). Resveratrol and pterostilbene share many pharmacological properties such as antioxidant, -inflammation, -cancer and -diabetes activity. One of the

metabolites of pterostilbene is 3'-hydroxypterostilbene which can be also isolated from the whole plant of the herb *Sphaerophysa salsula*.¹

As the stilbenes find application as pharmaceuticals and food supplements, a continuous high-volume industrial production is required for commercial applications. The methodology of flow chemistry is helpful to realize synthetic processes in continuous flow and is therefore described in more detail in the following section.

2.2 Flow Chemistry

As the production of resveratrol and its derivatives is aimed to be done continuously in a two-step chemo-enzymatic tandem reaction system, flow chemistry plays a major role in this thesis. Compared to conventional organic synthesis in batch, flow chemistry has many advantages, which allow to overcome problems and limitations of traditional processes for the production of the desired products.

Continuous flow reactors with channel diameters in the micro- and millimeter region have found widespread application in organic synthesis in the past few years. Especially the fine chemical and pharmaceutical industry is increasingly appreciating the advantages of continuous flow processing as the production of their products requires highly diverse and multiple production steps.¹⁴ Because of the high surface area-to-volume ratios, small-diameter flow reactors offer unique transport capabilities for matter and energy. An exquisite control of reaction temperature is possible as heat can be applied and removed more efficiently. This suppresses the formation of hot spots, temperature gradients or accumulation of heat, allowing the performance of fast and highly exothermic reactions.¹⁵ With this increased thermal controllability, solvent free production strategies become feasible, in this way saving up to 60 % of the overall energy consumption in the production of active pharmaceutical ingredients.¹⁶ Additionally, continuous flow systems are also beneficial for endothermic and slow reactions. The boiling point of solvents and reactants typically limits the reaction temperature. As flow systems can operate at high pressures these boiling points are shifted to higher temperatures compared to usual batch experiments conducted at atmospheric conditions. Likewise, yields and kinetics can be significantly increased as well using continuous flow technology.¹⁷ Furthermore, safety concerns can be minimized as thermal conditions and explosive atmospheres can be precisely controlled and risks associated with the handling of hazardous reagents can be reduced. Unstable or toxic synthetic intermediates can be generated in situ inside a closed system and converted directly into the desired non-hazardous product or intermediate. This allows the use of highly reactive and unstable chemicals, which could not be handled in batch processes.¹⁴ In contrast to perfectly mixed batch reactors, in small-diameter plug flow reactors the concentrations of reactants, intermediates and products are

resolved along the length of the reaction channel. This enables a precise control of the residence time and the process can be chemically or thermally quenched within the range of microseconds.¹⁸ Especially for industrial research and development, flow chemistry offers additional benefits. Typically, drug development is performed with quantities of the active pharmaceutical ingredient (API) in the order of grams or milligrams. After clinical and toxicological studies, which usually require kilograms of material, the successful pharmaceutical product needs to be produced on a hundred ton per year scale. Therefore, a scale up process over many orders of magnitudes is required. This scaling up is generally considerably easier for continuous than for batch processes. In this respect, often only minimal reoptimization and no major change of the synthetic pathway of optimized continuous laboratory routes is required. By simply using several flow devices or scaling up the reactor volume, the throughput can be increased, whereas the performance of the reactor can be conserved by keeping certain characteristics of the system constant (“smart dimensioning”).¹⁹

2.3 Chemo-Enzymatic Flow Set-ups

The combination of metal and biocatalysts has attracted increasing attention of researchers in the past decade. It unites the advantages of well-established catalyst technologies as well as enzyme catalysis and enables a new broad range of applications and novel processes. One-pot chemo-enzymatic synthesis combines the mild reaction conditions and extraordinary selectivity of enzymes and the versatility of traditional chemical catalysis.³ Heterogeneous metal catalysis combined with biocatalysts can avoid or reduce capacity-, time-consuming and waste-producing steps like purification and workup. This leads to superior processes in terms of sustainability and economic feasibility.²⁰

However, in a one-pot system several problems can occur, which are challenging or even impossible to solve. These issues can be mainly attributed to the incapability of the different employed catalysts. One-pot processes usually require a trade-off between the optimal conditions for each catalyst alone. The appropriate choice of solvent is crucial as most enzymes require aqueous systems for optimal activity, which in turn is problematic in terms of substrate solubility as well as hydrolysis of many chemo-catalysts. Further problems may arise like different optimum reaction temperatures and pH values, catalyst deactivation and poisoning.^{3,20}

Sequential flow setups can solve some of these problems as process parameters and conditions can be adapted and optimized for different spatial positions.²¹ Few examples of chemo-enzymatic continuous flow systems have been published in the recent years. In 2018, Farkas et al. published a lipase-mediated dynamic kinetic resolution to produce various enantiopure benzylic amines (Figure 2). Gel-immobilized lipase *Candida antarctica* B was used

as biocatalyst, which converts selectively the (*R*)-amine. As a racemic substrate mixture is used, a simple kinetic resolution would be limited to 50 % yield. Therefore, a heterogenous palladium catalyst was utilized to perform a redox racemization and an experimental yield of 96 % with an enantiomeric excess (*ee*) of 99 % was achieved. The catalytically active palladium was immobilized on a 3-aminopropyl- and 3-(2-aminoethylamino)propyl modified silica carrier and packed together with the gel-immobilized lipase in a mixed-bed stainless steel column reactor. As the redox racemization requires a hydrogen or ammonia source, a solution of ammonium formate had to be added after the first kinetic resolution with enzyme alone.²²

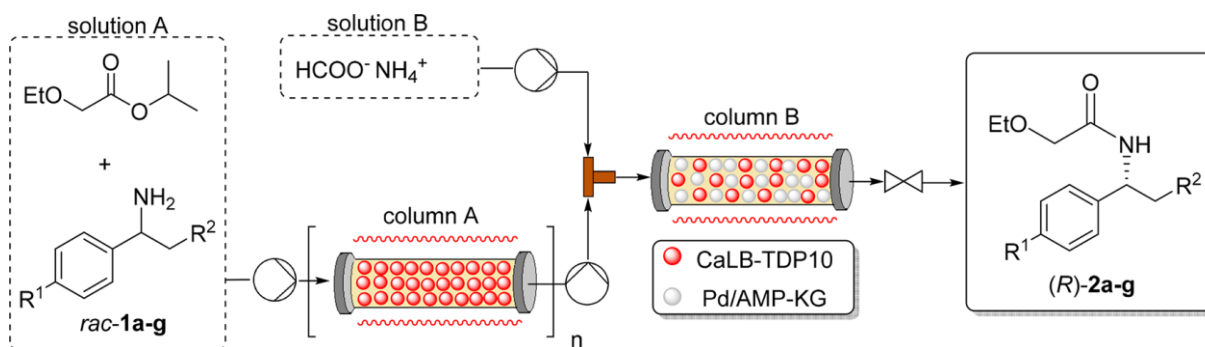


Figure 2 Continuous dynamic kinetic resolution to produce enantiopure amides (scheme reproduced from ²²)

Within this thesis, the development of a chemo-enzymatic continuous flow process for the synthesis of stilbene derivatives was targeted, which involves the cross-coupling of vinylphenol with aryl halides. This palladium-catalyzed C-C cross coupling reaction is named Heck reaction or Heck coupling and is described in more detail in the following chapter.

2.4 Heterogenous Heck Reactions

In 1972, Richard Fred Heck published the palladium-catalyzed coupling of olefins with aryl halides for the first time. Together with E. Negishi and A. Suzuki he was honored with the Nobel prize in chemistry for their achievements in the field of “palladium-catalyzed cross couplings in organic synthesis” in 2010.^{23, 24}

From a synthetic point of view, the Heck methodology provides several advantages such as high chemoselectivity, mild reaction conditions and low toxicity if appropriate catalyst removal techniques are applied. Therefore, metal catalyzed C-C couplings are omnipresent in synthetic organic chemistry and have revolutionized chemical synthesis. A large variety of olefins like derivatives of acrylates, styrenes or intramolecular double bonds are typically coupled with aryl bromides or iodides in the Heck type reaction. Additionally, also aryl sulfonyl chlorides, aromatic diazonium salts, aroyl anhydrides, aryl chlorides and arylsilanols are accepted as substrates. Generally, less crowded structures are preferred during Heck reaction and *trans*-products are favored. For the sequestration of generated acid, organic or inorganic bases like

alkali hydroxides or carbonates are usually added. Typically, dipolar aprotic solvents like *N*-methyl-2-pyrrolidone and *N,N*-dimethylformamide are beneficial for the reaction.²⁵ In recent years, extensive efforts were devoted to the adaption of the reaction conditions to aqueous media.²⁶ In this way, the combination of Heck coupling with enzymes, that usually prefer aqueous systems, to create chemo-enzymatic tandem reactions has become feasible. In 2020, Grabner et al. reported a deep eutectic solvent (DES) system that was successfully used for a combined Heck reaction/enzymatic decarboxylation using water and ethanol as co-solvents.³ With this solvent system, it was possible to overcome solubility problems of hydrophobic compounds and increase the substrate scope especially for continuous packed bed reactors that require a monophasic inlet flow. Together with Gavric they already optimized the solvent system for the particular problem of this thesis by mixing a DES:KPi 1:1 mixture for the decarboxylation with a DES:EtOH:H₂O = 1:6.75:2.25 as iodoaryl solvent. The resulting mixture for the Heck coupling step was DES:Buffer KPi:H₂O:EtOH = 6:5:2.25:6.75 (v/v).^{3, 4}

Usually, palladium is the preferred transition metal to catalyze Heck reactions. While in the beginnings of C-C cross-coupling mainly homogenous catalysts like palladium phosphine complexes were used, heterogenous systems have been increasingly desired and developed. Especially for industrial applications and continuous processing, these heterogenous systems are highly beneficial as the separation and recycling of homogeneous organometallic catalysts is a great challenge. It requires expensive nanofiltration membranes or a tedious column chromatography step. For the production of pharmaceutical products, the maximum acceptable concentration of transition metals is further an issue that needs to be concerned (Table 1).²⁷ Compared to batch reactions, the use of packed-bed microreactors allows a high local concentration of catalyst and, due to enhanced mass transfer, higher turnover numbers and reaction rates are feasible.²⁸

Table 1 Maximum acceptable concentrations limits for residues of metal catalysts for pharmaceuticals²⁷

Metal	Oral	Parenteral
	Concentration [ppm]	
Pd, Pt, Ir, Rh, Ru, Os	5	0.5
Mo, V, Ni, Cr	10	1.0
Cu, Mn	15	1.5
Zn, Fe	20	2.0

While the catalytic mechanism of homogenous systems is well understood, for heterogenous systems the situation is different.²⁷ In Figure 3, the mechanism of homogenous palladium catalysis in presence of a ligand as well as the pseudo-heterogenous concept of “ligandless” catalysis are depicted. Regardless of the concept, the catalytic cycles consist of the same

three steps: 1) oxidative addition, 2) transmetalation and 3) reductive elimination.²⁸ There are still many debates about the true nature of the active palladium species in a reaction employing nominally heterogeneous palladium catalysts. While some authors claim to have developed truly heterogeneous systems with catalysis taking place on the solid catalyst surface, others consider the solid pre-catalyst as a reservoir of soluble catalytically active palladium species.²⁷ Supporters of the last-mentioned theory argue that significant leaching of the metal from the solid matrix almost inevitably occurs. The mechanistic transformation of Pd⁰ into a soluble Pd^{II} species further supports the idea of a quasi-homogeneous intermediate. After completion of the catalytic cycle, Pd⁰ typically redeposits onto the support in a batch experiment but the transition metal will be progressively “chromatographed” through the packed-bed catalyst in a continuous setup. This leaching process decreases the catalytic activity and could contaminate the product stream with the metal (Table 1).²⁸

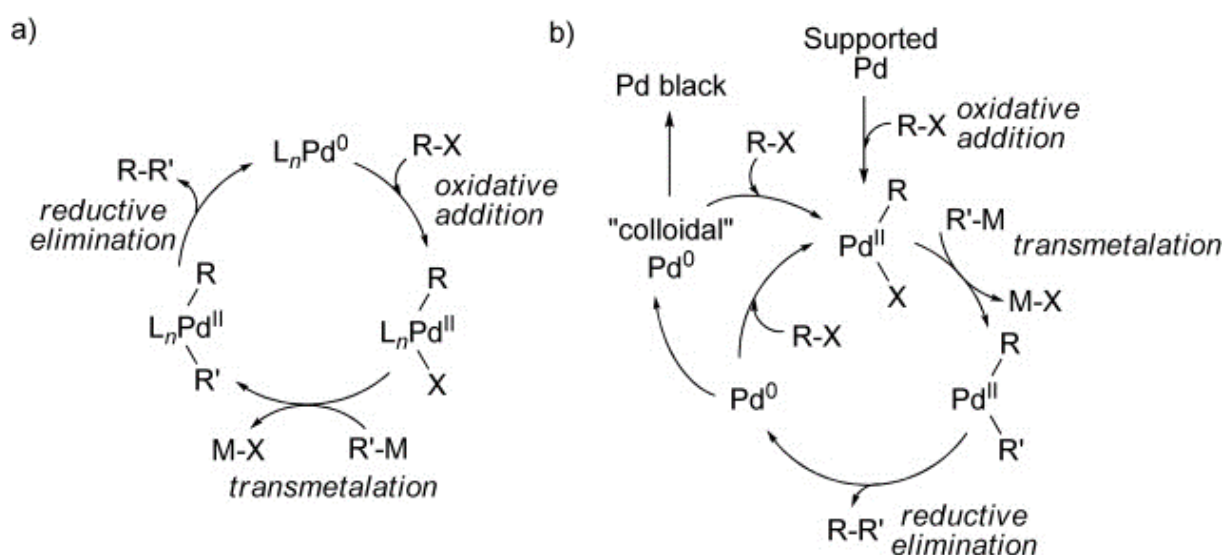


Figure 3 Catalytic cycles of Heck reaction using a) homogeneous palladium in the presence of a ligand, and b) the concept of “ligandless” palladium catalysis (reproduced from²⁸)

In general, for supported metal catalyst systems, the most common chemical or physical immobilization principals are based on the of covalent bonding, ionic bonding, adsorption and encapsulation. For the pallidum in particular different heterogenous palladium catalysts have been published in the recent years, which differ in the immobilization technique as well as application and can be divided into two different groups.²⁸

The first group are immobilized ligand-free transition metals. Palladium can be immobilized on different supports like carbon/graphite/graphene, simple inorganic materials (silica, alumina), or sophisticated tailor-made supports such as monolithic materials or polymers. Regarding the latter, one example is the development of a monolithic flow reactor comprising polymer-bound palladium. The solid support was produced via precipitation polymerization of monomers like vinylchlorobenzene and divinylbenzene. Obtained small polymeric beads were then crosslinked and transformed into quaternary ammonium ions. To load the monolith-based reactors with

Pd^0 nanoparticles, an ion-exchange was performed followed by a reduction.²⁸ Apart from that, another class of heterogeneous Pd catalysts has to be mentioned due to its importance for this thesis. As reported by Lichtenegger et al. in 2016, metal oxide supported ionic palladium catalysts of formula $\text{Ce}_{0.99-x}\text{Sn}_x\text{Pd}_{0.01}\text{O}_{2-\delta}$ ($x=0-0.99$) can be synthesized easily and fast with a solution combustion method in different stoichiometric ratios. For the synthesis of these nanocrystalline mixed oxides, glycine is used as combustion fuel and mixed together with appropriate amounts of ammonium cerium(IV) nitrate, tin(II) oxalate, palladium(II) chloride as well as water and ignited at 350 °C in an oven. With this method, highly active catalysts with a turnover frequency above 12,000 h^{-1} for Suzuki couplings could be produced. Due to the high catalyst stability, reactions were carried out at atmospheric conditions and aqueous ethanolic solutions were used as solvents. Furthermore, only minimal leaching of less than 0.14 mg/L palladium in the product solution was reported for certain substrates during continuous flow experiments. Due to the reaction kinetics and catalyst poisoning tests the authors support the thesis of a homogenous reaction mechanism involving dissolved palladium species. However, the catalyst could be reused for at least five times without a significant change in activity or crystal structure.²⁹

The second group of heterogeneous palladium catalysts are formed via immobilization of the transition metal by ligands, which are chemically bound to a solid support. Ligand coordination usually modifies the activity and therefore might increase the reactivity of the catalyst. In most cases, the ligands are covalently bound to a solid support to immobilize the ligand metal complex. Common ligands for palladium are phosphines, *N*-heterocyclic carbenes or salen-type ligands. Various supports like silica, polymers or sol-gel entrapped systems are possible.²⁸

Apart from a Heck reaction facilitated by heterogeneous Pd-Ce-Sn-oxides, the enzymatic decarboxylation of coumaric acid is a key step of the chemo-enzymatic continuous tandem reaction targeted within this thesis. This type of transformation as well suitable biocatalysts are presented in the following.

2.5 Coumaric Acid and Enzymatic Decarboxylation of Phenolic Acids

p-Coumaric acid represents the starting material of aimed tandem reaction reported in this thesis and is decarboxylated in the first step of the continuous process for the synthesis of stilbene. This enzymatic reaction is catalyzed by a phenolic acid decarboxylase (PAD) from the bacterial strain *Bacillus subtilis* and immobilized to be applicable in continuous flow systems.

A variety of phenolic acids are abundant and naturally occurring in plant cell walls, facilitating linking of the lignin polymer to hemicellulose as well as cellulose and contribute therefore to the rigidity of plants. One representative of this group is *p*-coumaric acid, present in soluble form in the cytoplasm as well as covalently bond to plant cell walls. Many organisms contain enzymes named cinnamoyl ester hydrolases, that give them the ability to hydrolyze these ester bonds and produce coumaric acid in its free form from lignin and hemicellulose. This allows the production of coumaric acid from renewable resources and waste products from the paper and pulp industry can be used to generate this fine chemical.^{30 31}

The non-oxidative enzyme phenolic acid decarboxylase can be found in various microorganisms like *Saccharomyces cerevisiae*, *Bacillus pumilus*, *Bacillus subtilis* or *Lactobacillus*.³¹ For the last-mentioned bacteria, the enzymatic two-step mechanism was intensively studied and published by Rodriguez et al. The first step is binding of the substrate *p*-coumaric acid to the enzyme via the unprotonated carboxyl group, which explains the influence of the pH-value on the enzymatic transformation. The catalytic mechanism starts with deprotonation of the phenolic hydroxy group by the carboxylate anion of Glu71, promoting an electron flow along the cinnamate structure. This mechanism leads to a *para*-quinone methide intermediate, which promotes a second electron flow from the carboxylate, releasing CO₂. For this second step, water serves as proton source and was identified to be present in the internal cavity (Figure 4).³¹

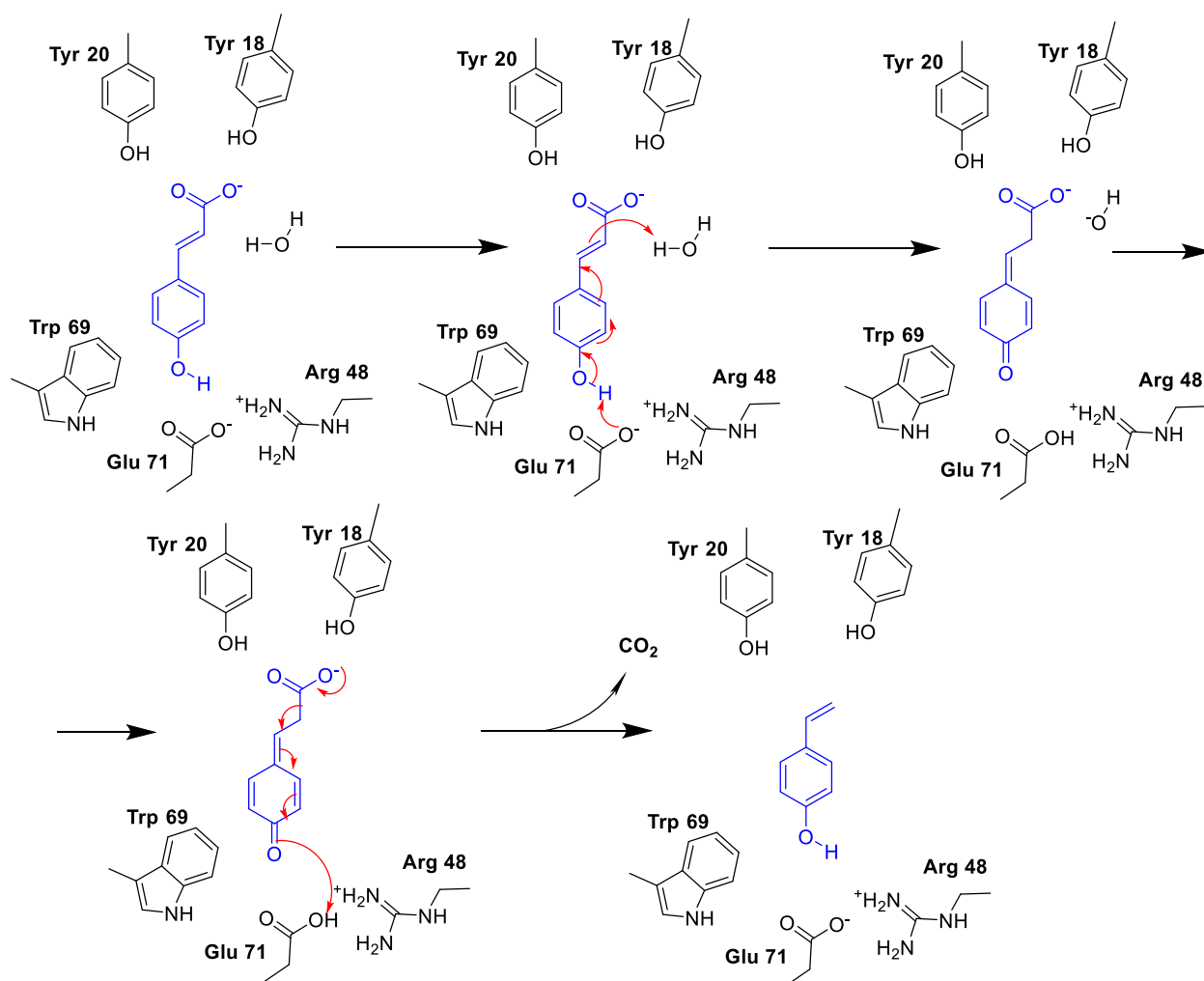


Figure 4 Enzymatic decarboxylation mechanism catalyzed by *Lactobacillus phenolic acid decarboxylase* (target molecule in blue, reproduced from ³¹)

Especially the cofactor-free phenolic acid decarboxylase (*BsPAD*) from *B. subtilis* has already been shown to be a robust and suitable biocatalyst and is therefore used in this thesis. It is produced in lab scale by cloning genomic DNA, soluble expression and purification. According to Gomez Baraibar et al., a yield of 40 mg of semi purified *BsPAD* could be obtained from 1 g cell pellet. In a 50 mM KPi-buffer system with pH 6.0 at 30 °C, a specific enzyme activity of $312 \pm 40 \text{ U mg}^{-1}$ for *p*-coumaric acid as substrate could be achieved.³² Furthermore, this *BsPAD* enzyme shows excellent activity in deep eutectic solvents, which increases its usability and scope as hydrophobic substrates and products can be dissolved in higher concentrations and monophasic solutions can be used.³

2.6 Enzyme Immobilization

In order to employ enzymes for continuous flow set-ups, a special fixation is necessary. Similar to transition metal catalysts, an immobilization is required to receive a heterogeneous catalyst. However, the methods differ substantially due to the nature of enzymes.

For the production of an immobilized enzyme system, usually a suitable matrix, a mode of attachment and the enzyme itself are required. To attach enzymes to a solid support, various interactions ranging from reversible physical adsorption, affinity binding to ionic bonding are applied. Furthermore, irreversible but very stable covalent bonds that are present as amide, carbamate, ether or thioether could be used. To maintain the activity of the enzyme not only the appropriate choice of bonding but also an appropriate support is necessary. In theory, ideal supports should have properties like hydrophilicity, inertness towards enzymes, resistance to microbial attack, biocompatibility and accessibility at a low cost. Additionally, the availability for reactive functional groups, mechanical stability, non-toxicity and biodegradability are desired. According to their chemical composition, supports can be classified into organic or inorganic and further into natural or synthetic polymers. The most common support materials are starch, collagen, carboxymethyl-cellulose, modified sepharose, ion exchange resins, active charcoal, aluminum oxide, agarose, silica, alginate and certain polymers.³³ The versatile immobilization technique entrapment is of special interest for this thesis as it used to encapsulate the *BsPAD* enzyme with sodium alginate. The idea of entrapment technologies is to enclose microorganisms or enzymes in a rigid network to prevent the release of the active substance into the surrounding media. This network is produced via a physical or chemical polymerization process to create a barrier that is porous enough to allow diffusion of substrates and products. The simplest and most common method of enzyme entrapment is the gelation of polyanionic or cationic polymers by the addition of multivalent counterions like Ca^{2+} or Ba^{2+} . As polymeric matrix, various polymers like collagen, polyacrylamide, gelatin, polyurethane, silicon rubber or polyvinyl alcohol find application. However, alginates are most frequently used due to their versatility, non-toxicity and the fact that they allow mild reaction conditions (Figure 5). The production of insoluble entrapped enzyme beads is easily done by mixing water-soluble alginate with the enzyme or microorganism and dropping them into a counterion solution e.g. CaCl_2 . Nevertheless, entrapment technologies tend to have mass transfer limitations and suffer from enzyme leaking compared to other technologies.^{33, 34}

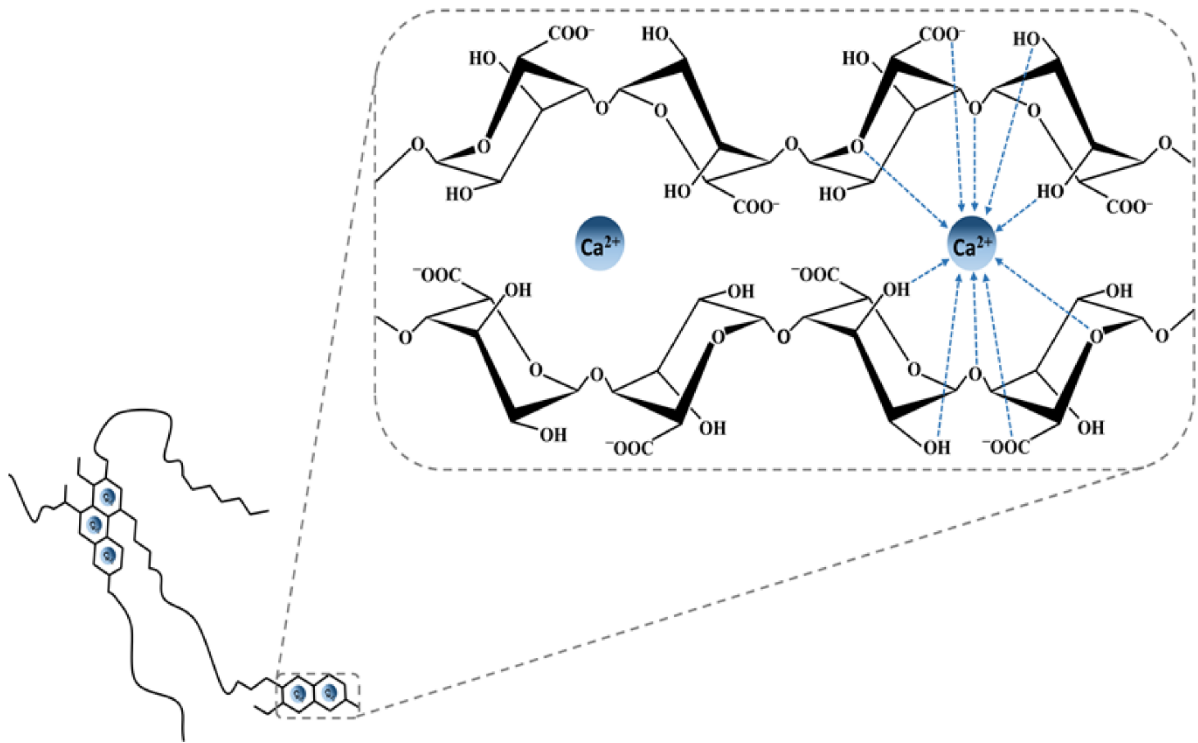
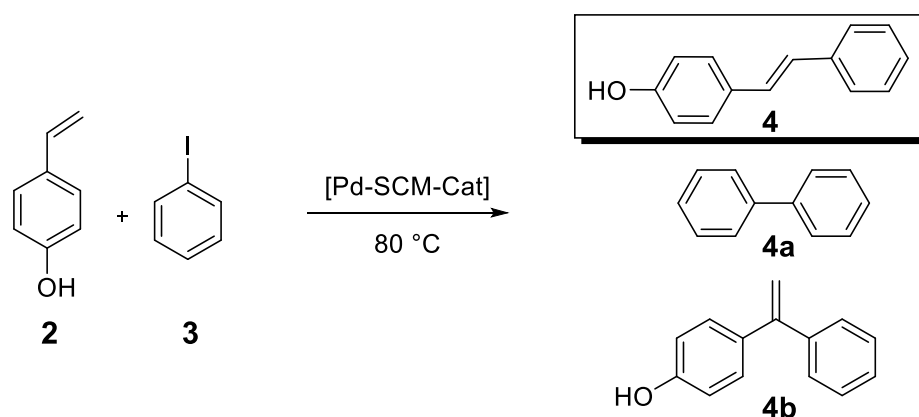


Figure 5 Na-alginate encapsulation with Ca^{2+} -Ions (reproduced from ³⁵)

3 Results and Discussion

3.1 Optimization of Process Conditions in Batch

To evaluate which parameters influence yield and byproduct formation in the Heck reaction, various batch experiments were conducted according to chapter 4.3.5 and Scheme 1, testing different pH-values and carbonate concentrations. It turned out that only hydroxystilbene **4** could be synthesized in batch mode, whereas structurally similar stilbenes **6** and **8** were not formed at a reaction temperature of 80 °C, which was limited by the boiling point of the solvent. Therefore, only the cross coupling step for the synthesis of hydroxystilbene **4** was optimized in batch and identified optimal reaction parameters were also applied for the synthesis of **6** and **8**. While solvent composition (DES:Buffer(KPi):H₂O:EtOH = 6:5:2.25:6.75) and molar equivalents (1 mol eq. of **2**, 1.5 mol eq. of **3**) of the substrates were already optimized by Kristian Gavric⁴, variation of pH-value and carbonate concentration were promising to further optimize the reaction. These two parameters were varied independently between 0-100 mM K₂CO₃ and pH-value 10.5-13 along with vinylphenol **2** concentrations between 10-40 mM. This wide range of vinylphenol **2** substrate concentration was necessary to evaluate if the optimized parameters are related to substrate concentrations or required as absolute concentrations. To get comparable and reproducible results, all the other reaction parameters such as solvent, molar equivalents of reagents, temperature, sampling procedure and catalyst mass remained constant. While it was aimed to maximize the yield of hydroxystilbene **4**, the concentration of byproduct **4b**, formed due to a different regioselectivity in the coupling reaction, should be minimized. The parameter DP/SP (desired product **4**/side product **4b**) was introduced to describe the ratio of HPLC peak areas of the desired product **4** to the byproduct **4b**. In contrast to the high temperature flow experiments, homocoupling of iodobenzene **3** was not observed in any batch experiment.



*Scheme 1 Heck coupling experiments in batch using standard batch conditions according to chapter 4.3.5; substrates: vinylphenol **2**, iodobenzene **3**; products: hydroxystilbene **4**, biphenyl **4a**, para-hydroxy-1,1-diphenylethylene **4b**; catalyst produced with solution combustion method (SCM)*

3.1.1 Optimum pH-value

Besides temperature, basicity turned out to have the most significant effect on the product yield. Regardless of the vinylphenol **2** concentration, all batch experiments showed the same trend and an optimum pH-value range between 11.5-12 could be determined experimentally, which is visualized in Figure 6. The pH-value was set by adding KOH while measuring with a pH-meter. Beyond this optimum pH window, the yield decreased fast. Especially at high pH-values of 13 or more, almost no product was formed. Also, at a low pH-value of 10.5, the average yield decreased more than 42 %.

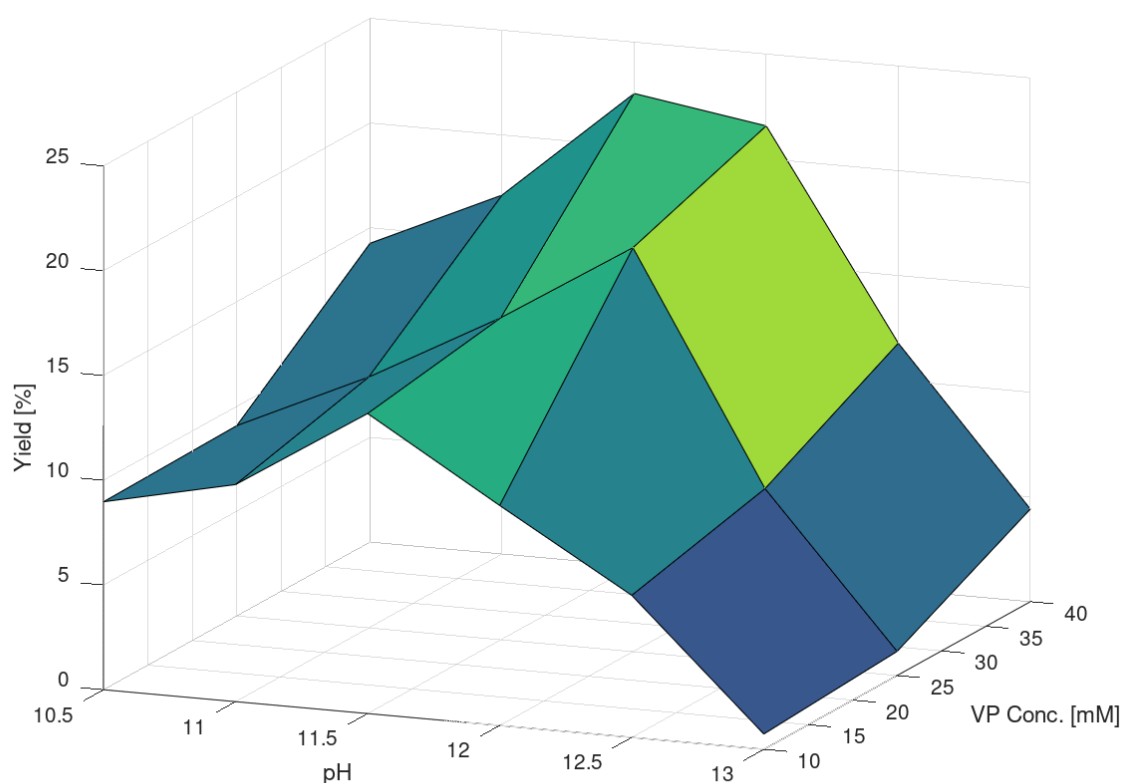


Figure 6 Surface plot of pH-value and vinylphenol (VP) **2** concentration influencing product yield; batch experiments according to chapter 4.3.5

The relationship between pH-value, vinylphenol **2** concentration and DS/SP ratio is visualized as surface plot in Figure 7. The optimum pH range is again between 11.5-12. This behavior can mainly be explained by the increased formation of product **4** in this pH range, whereas the formation of byproduct **4b** turned out to be rather constant over the analyzed pH range.

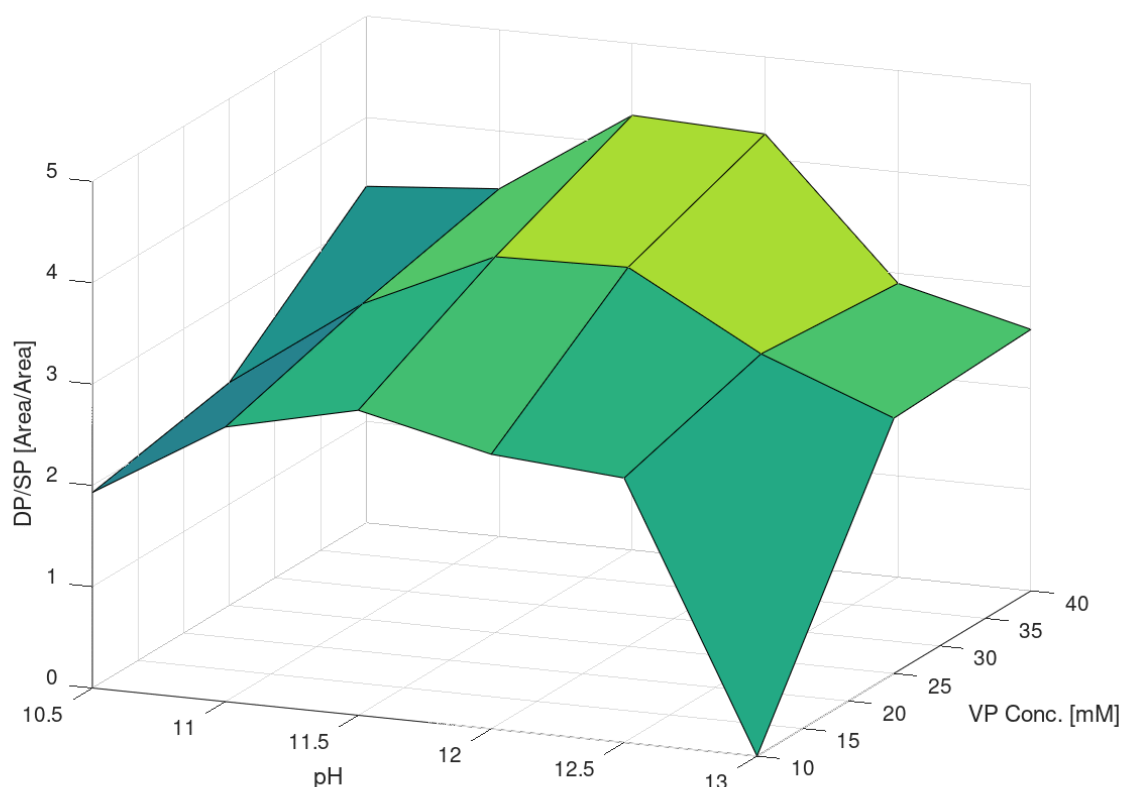


Figure 7 Surface plot of pH-value and vinylphenol (VP) **2** concentration influencing DP **4**/SP **4b** peak area ratio; batch experiments according to chapter 4.3.5

3.1.2 Optimum Carbonate Concentration

While the KOH concentration and consequently the pH-value showed to have only minor influence on the formation of byproduct **4b**, the concentration of carbonate plays a significant role. Keeping the pH-value constant at 11.75, the influence of K_2CO_3 on yield and DP/SP ratio is depicted in Figure 8. Regardless of the vinylphenol **2** concentration, less byproduct **4b** was formed at higher carbonate concentrations, which led to increasing DP/SP ratios. Unfortunately, the opposite trend was revealed for the yield. With increasing amounts of K_2CO_3 , the yield decreased. However, for high concentrations of substrate **2** only 15 mM carbonate were required. Therefore, regarding the carbonate concentration, a compromise needed to be found in order to obtain decent yields but still have acceptable low amounts of byproduct **4b**. As high yields were the predominant goal of this thesis, a concentration of 15 mM K_2CO_3 was used for the following experiments.

With the new optimized process conditions of pH 11.75, adjusted by KOH addition, and 15 mM K_2CO_3 a yield of 12.4 % and 22.1 % could be obtained for vinylphenol **2** concentrations of 10 and 40 mM, respectively. The desired product **4** to side product **4b** ratios (DP/SP) were 2.86

and 4.26 for these conditions. Compared to conditions used in the previous work⁴ 1.5 mol eq. K_2CO_3 and 10 mM **2**, the yield obtained in batch experiments could be increased by 38 %.

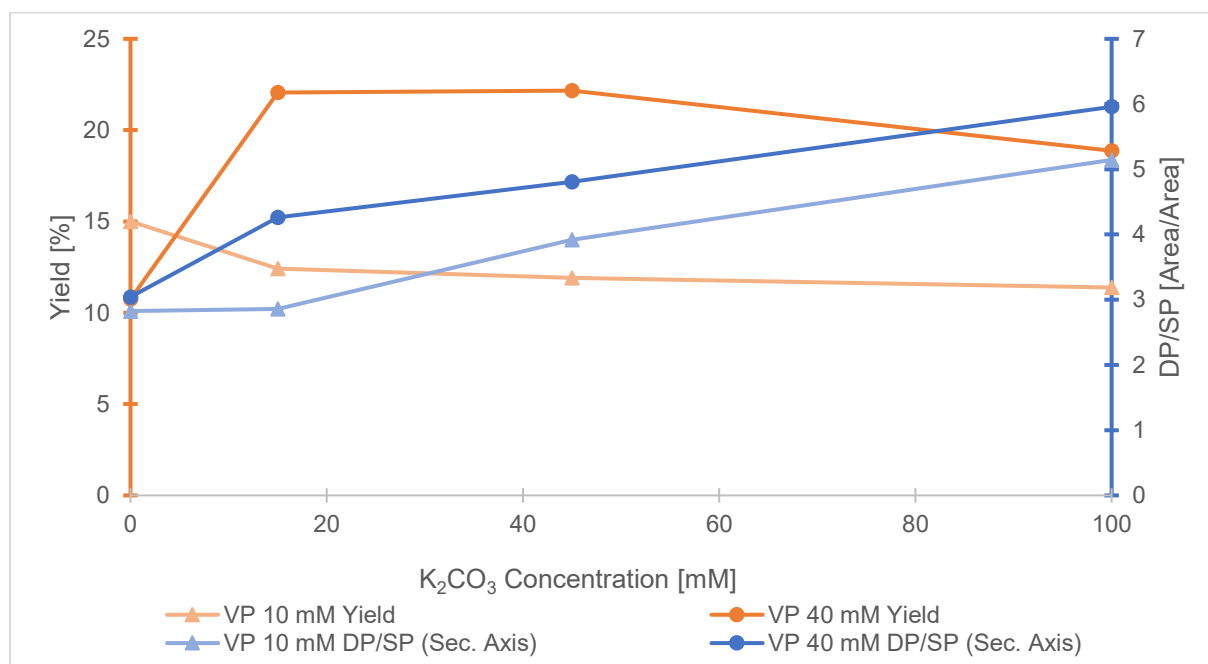
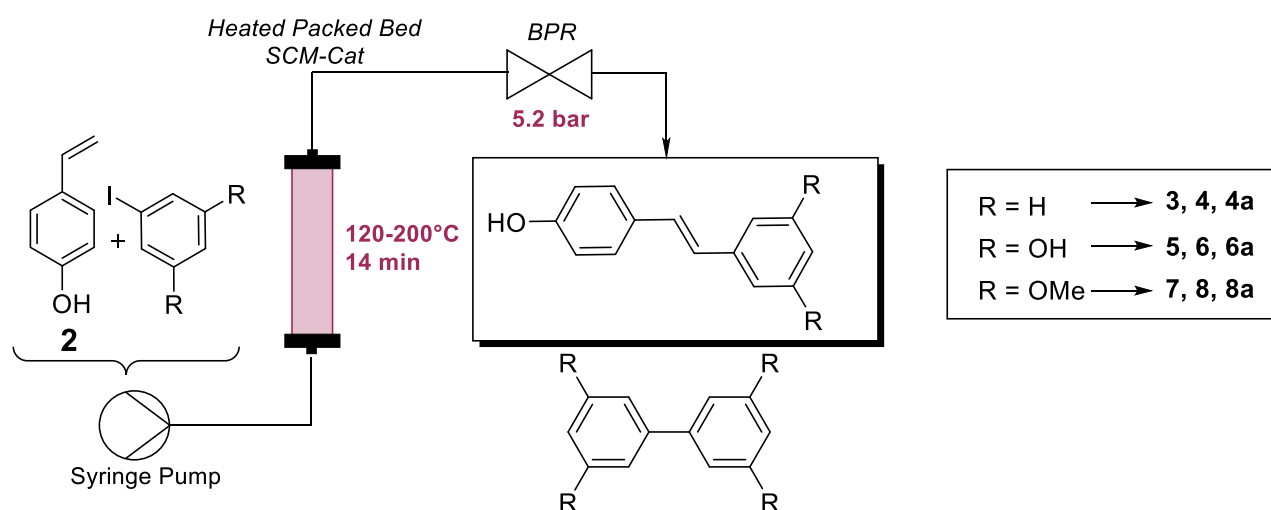


Figure 8 Influence of K_2CO_3 concentration on yield (orange) and DP **4**/SP**4b** peak area ratio (blue) with two different vinylphenol **2** concentrations and constant pH of 11.75; batch experiments according to chapter 4.3.5.; for better visualization points are connected

3.2 Heck coupling in Continuous Flow

Before the full chemo-enzymatic tandem experiment was carried out, several experiments studying the Heck coupling reaction alone in continuous flow were conducted, as this step was shown to be the bottleneck of the cascade. While the enzymatic decarboxylation step gives full conversion and almost quantitative yield, the yield of the palladium catalyzed step was reported to be only around 20 % in previous works.⁴ Furthermore, resveratrol **6** and pterostilbene **8** could only be synthesized in flow or autoclaves as temperatures higher than 80 °C were required, which exceeds the boiling point of the solvent at ambient pressure. To benefit from the advantage of flow chemistry to heat above the boiling point of the reaction mixture, a backpressure regulator (5.2 bar) was installed. With the elevated system pressure, the reactions could be run at temperatures up to 200 °C without bubble formation. In Scheme 2 and Table 2, the routes to synthesize the three different products **4**, **6** and **8** as well as the

homocoupling byproducts are depicted. While vinylphenol **2** from commercial sources was used as substrate for all experiments, the iodoaryl coupling partner **3**, **5** and **7** was varied.



Scheme 2 Continuous Heck coupling experiments; different substrates and process conditions were used according to Table 2 and Table 3; flow experiments conducted according to chapter 4.4.1.; base was added to substrate mixture

Table 2 Substrates, products and homocoupling side products used and synthesized in continuous Heck coupling experiments

Residue	Iodosubstrate	Product	Homocoupling Product
R = H	iodobenzene 3	4-hydroxystilbene 4	biphenyl 4a
R = OH	2,4-dihydroxyiodobenzene 5	resveratrol 6	[1,1'-biphenyl]-3,3',5,5'-tetraol 6a
R = OMe	2,4-dimethoxyiodobenzene 7	pterostilbene 8	3,3',5,5'-tetramethoxy-1,1'-biphenyl 8a

The conditions used for the experiments as well as analyzed parameters are summarized in Table 3. Not listed in this table are the experimental parameters (15 mM K_2CO_3 , pH 11.75, ~1.6 g Pd-Solution Combustion Method (SCM) catalyst (10.3 mmol SCM-Cat, 1 mol% Pd), solvent DES:KPi:H₂O:EtOH = 6:5:2.25:6.75) that remained unchanged throughout all flow experiments. From the batch experiments described in chapter 3.1, a pH-value of 11.75 and a K_2CO_3 concentration of 15 mM were evaluated to be optimal. Furthermore, always the same stainless-steel catalyst column with almost the same catalyst amount and a system pressure of 5.2 bar were used. All experiments were conducted as described in chapter 4.4.1. The parameter with the most significant impact on product as well as byproduct formation was determined to be the temperature. Therefore, in every experiment different temperature ramps

were tested to get information about the influence of this parameter on the formation of different species as well as catalyst stability and degradation.

Table 3 Experimental parameters and analyzed parameters of continuous Heck coupling reactions according to chapter 4.4.1

Entry	Educts	Temperature [°C]	Flow rate [mL/min]	Purpose/Analyzed Parameter
1	10 mM 2 15 mM 3	80,90,100,110	0.1	Pd-leaching for ICP-MS, temperature
2	20 mM 2 30 mM 5	130,160	0.2,0.4	resveratrol production, flow rate
3	10 mM 2 15 mM 3	140,160,170,180,200	0.2	temperature
4	10 mM 2 15 mM 5	140,150,160	0.2	cat. stability
5	20 mM 2 30 mM 7	120,140,160	0.2	pterostilbene production temperature, cat. stability

3.2.1 Continuous Synthesis of Hydroxystilbene **4**

As hydroxystilbene **4** has already been synthesized, characterized and calibrated for HPLC measurements in previous work, the main goal was optimization of the reaction temperature, which was varied between 80 and 200 °C.⁴ In Figure 9, reactants and product concentrations as well as the temperature profile over time are plotted. A clear trend of increased formation of desired product **4** with higher temperature becomes evident with a maximum at 170 °C. At higher temperatures, yield decreased drastically. At the temperature optimum of 170 °C, a yield of 53.6 % was achieved. However, it is very likely that not the real temperature optimum of the reaction was found. Catalyst stability experiments suggest that the sharp decrease in product concentration was caused by a loss of catalyst activity at high temperatures and not by the reaction kinetics itself. High biphenyl **4a** concentrations and lower vinylphenol **2** conversion at temperatures above 170 °C support the assumption of catalyst degradation. The relationship between catalyst degradation and increased homocoupling could be observed throughout this thesis. The formation of the side product **4b** increases simultaneously with hydroxystilbene **4** and therefore, the ratio DP (**4**) to SP (**4b**) of around 4.3 remains relatively constant over time and temperature.

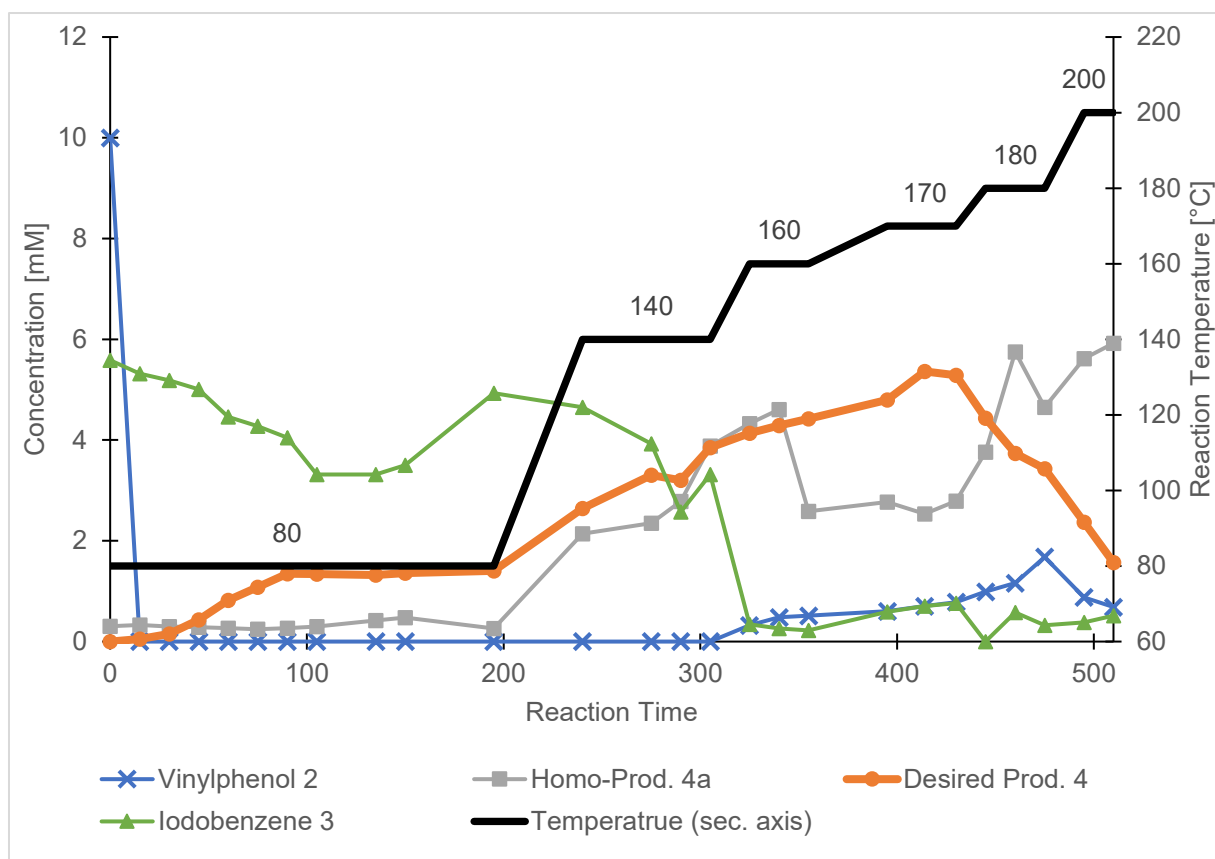


Figure 9 Heck reaction in continuous flow for formation of hydroxystilbene **4**; concentrations of vinylphenol **2** (blue), homocoupling product **4a** (grey), hydroxystilbene **4** (orange) and iodobenzene **3** (green) over reaction time; temperature profile (black) on secondary axis; experiment conducted according to chapter 4.4.1 with 10 mM of **2**

3.2.2 Continuous Synthesis of Resveratrol **6**

Before the actual coupling experiments could be carried out, the iodoaryl substrate 2,4-dihydroxyiodobenzene **5** was synthesized as described in chapter 4.3.6. For the two-step one-pot synthesis, the cheap and commercially available phloroglucinol was used as substrate. After the regioselective single amination with ammonia, a diazonium salt was formed using NaNO_2 . After a Sandmeyer-like reaction using potassium iodine, obtained iodoaryl substrate **5** was purified via column chromatography and obtained in a moderate yield of 24.8 %.

The Heck coupling experiment in continuous flow was conducted using similar conditions as reported for hydroxystilbene **4** but with a modified temperature profile, as can be seen from Figure 10. The initial temperature was set again at the end of the experiment to study the influence of catalyst degradation. Using this experimental setup at 160 °C, resveratrol **6** could be synthesized with a maximum yield of 24.5 %. While vinylphenol **2** was never fully converted during the experiment, the iodoaryl substrate **5** reacted completely, although it was used in 50 % molar excess. This finding correlates with the substantial homoproduct formation **6a** at the beginning of the experiment. Product concentrations were rather constant for 300 minutes but decreased significantly after changing the temperature to 160 °C. The sharp decrease of

product yield as well as conversion goes along with an increase of homoproduct formation **6a** and was caused by catalyst degradation. Comparing the reaction temperature of 150 °C at the beginning as well as at the end of the experiment, a decrease of product concentration of more than 300 % further supports the theory of catalyst degradation. Unfortunately, neither the influence of temperature nor the optimal temperature could be evaluated due to this effect.

During the flow experiment, the product stream was collected and the product resveratrol **6** could be isolated, purified and characterized via $^1\text{H-NMR}$ and $^{13}\text{C-NMR}$.

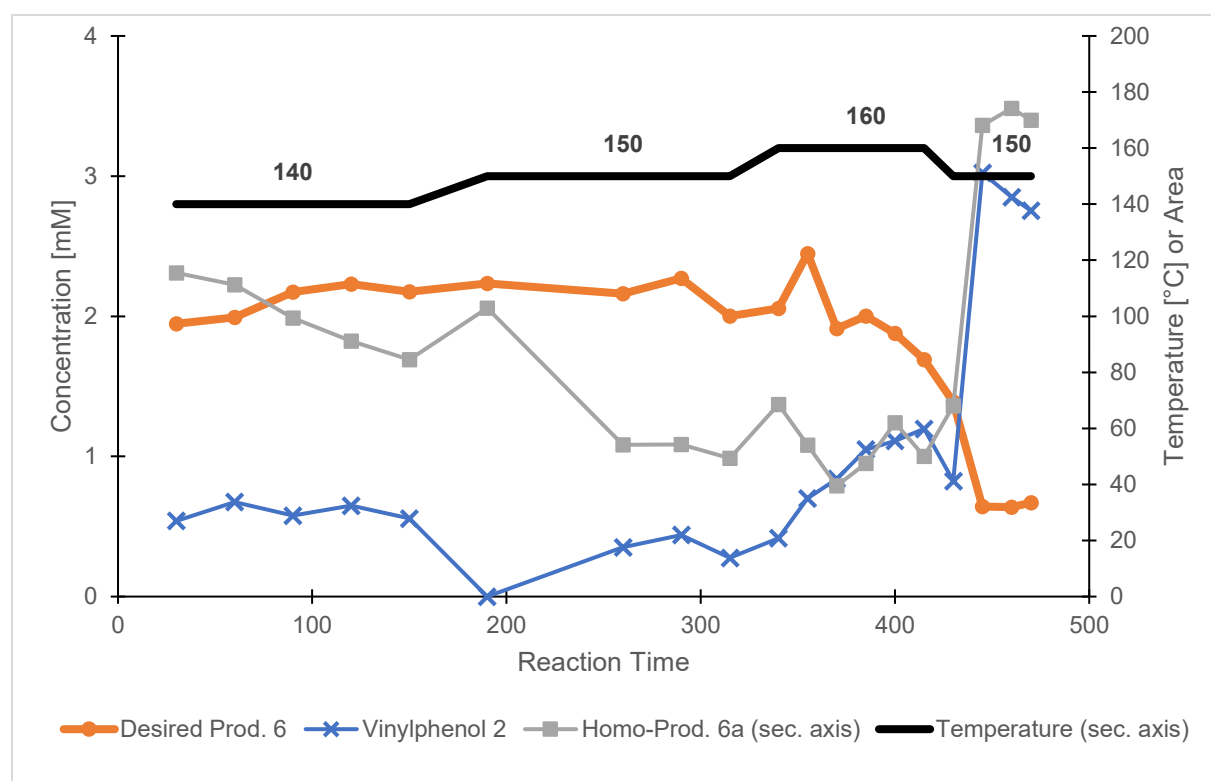


Figure 10 Heck reaction in flow for synthesis of resveratrol **6**; concentrations of vinylphenol **2** (blue), homocoupling product **6a** (grey) and resveratrol **6** (orange) over reaction time; temperature profile (black) on secondary axis; experiment conducted according to chapter 4.4.1 with 10 mM of **2**

3.2.3 Continuous Synthesis of Pterostilbene **8**

Similar to the continuous synthesis of resveratrol **6**, the iodoaryl substrate **7** needed to be synthesized first in order to be able to synthesize pterostilbene **8** in continuous flow. However, as commercially available starting material 3,5-dimethoxy-1-aniline was used, the amination step was not necessary according to chapter 4.3.7. The required diazonium salt was formed using NaNO_2 followed by a Sandmeyer-like reaction to introduce the iodo-group. After purification via column chromatography, the pure substrate was obtained in a moderate yield of 22.6 %.

The continuous flow experiment for the synthesis of pterostilbene **8** was conducted at three different temperatures with setting the temperature to the start value again at the end. In contrast to the other two continuous Heck coupling experiments, no significant catalyst degradation could be observed this time. The reaction yield at a temperature of 120 °C at the beginning as well as the end of the experiment only differed slightly and formation of homoproduct was only affected by the reaction temperature and not by the reaction time. Stable product formation was observed at a reaction temperature of 140 °C with a maximum yield of 50.2 %. While the iodoaryl substrate **7** was fully converted at temperatures above 140 °C, the conversion of the limiting reagent vinylphenol **2** never exceeded 81 %. This could be probably explained by a higher affinity of **7** for homocoupling and correlates with the measured homoproduct formation **8a**.

During the flow experiment, the product stream was collected and the product pterostilbene **8** could be isolated, purified and characterized via $^1\text{H-NMR}$ and $^{13}\text{C-NMR}$.

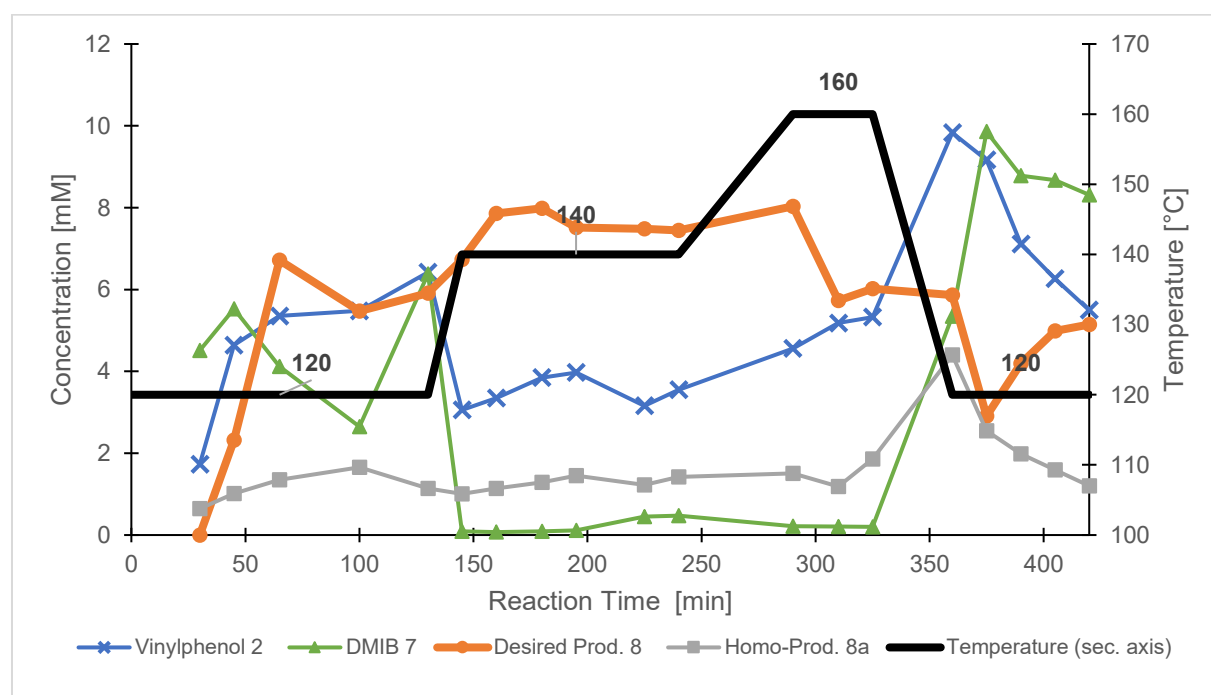
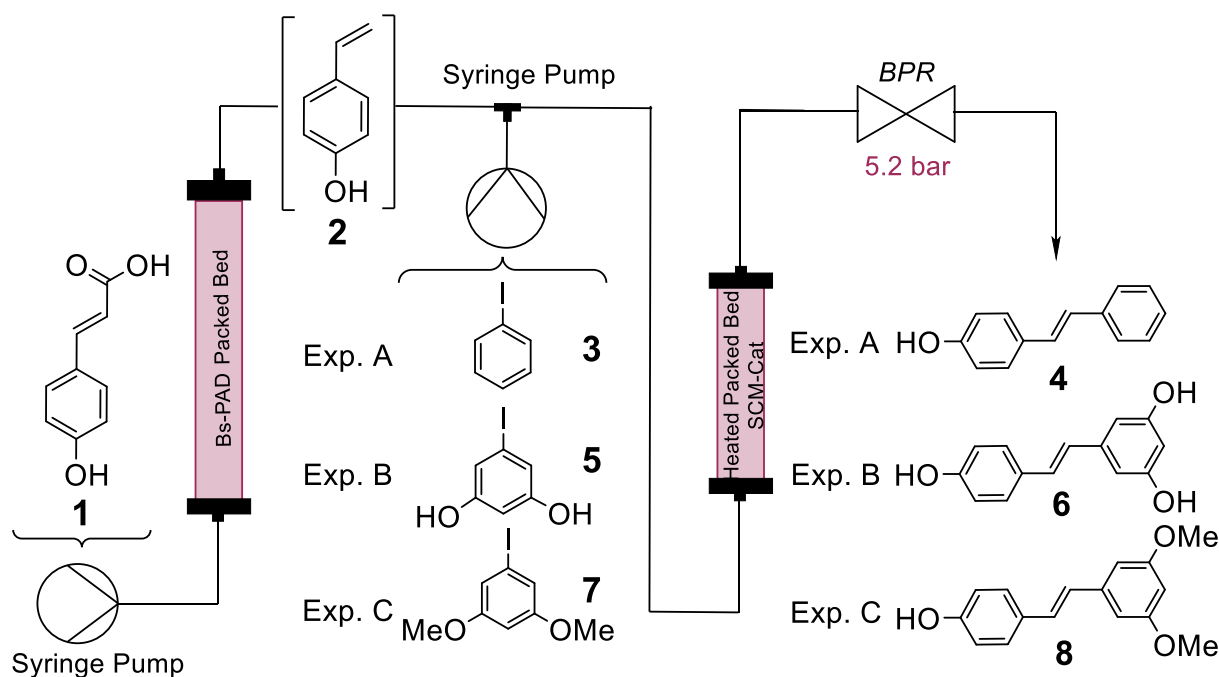


Figure 11 Heck reaction in flow for synthesis of pterostilbene **8**; concentrations of vinylphenol **2** (blue), homocoupling product **8a** (grey), pterostilbene **8** (orange) and 2,4-dimethoxyiodobenzene **7** (green) over reaction time; temperature profile (black) on secondary axis; experiment conducted according to chapter 4.4.1 with 10 mM of **2**

3.3 Tandem Flow Experiments

In the tandem experiments, the two steps of the targeted cascade (enzymatic decarboxylation followed by the metal-catalyzed Heck coupling) were combined, representing the full process for the synthesis of stilbenes (Scheme 3). The starting substrate coumaric acid **1**, dissolved in buffer and deep eutectic solvent, was pumped through a bed of immobilized enzyme giving the intermediate compound vinylphenol **2**. The stream was then mixed with the corresponding iodoaryl substrate as well as base to perform the intermolecular coupling and obtain the final product. While in preliminary experiments a lot of effort was put into the optimization of the second part of the reaction cascade, the enzymatic decarboxylation worked with full conversion and quantitative yield throughout this thesis. For the metal catalyzed part, optimized process conditions as mentioned in chapter 3.2 were used comprising 145 °C reaction temperature, 15 mM K₂CO₃, 22 mM KOH, 15 mM iodoaryl substrate and a flow rate of 0.2 ml/min according to 4.4.2. These parameters were kept constant for all substrates as it was intended to demonstrate the stability of the process over time. To maintain the stability of the catalyst for at least 300 minutes, a compromise between high yield and catalyst degradation needed to be made as both parameters increase with higher temperature. Before the whole tandem setup was used, the decarboxylation step was also tested alone but always showed full conversion. Following a short start-up phase of 30-60 minutes, it provided quantitative product yield for more than 12 hours. After change of the iodoaryl substrate, a column packed with fresh SCM catalyst was used. The mean residence time of the entire setup was determined to be 38.5 minutes and was measured in a separate experiment according to chapter 4.4.3.



*Scheme 3 Tandem flow experiment comprising enzymatic decarboxylation as well as Heck coupling of vinylphenol with various iodoaryl substrate to give stilbenes; ; first syringe pump(left) provides a 20 mM coumaric acid **1** solution in DES:KPi 1:1 for the decarboxylation column filled with 160 mg BsPAD immobilized in enzyme beads; the product vinylphenol **2** is coupled with various iodoaryl substrates **3**, **5** and **7** dissolved in DES:EtOH:H₂O 1:6.75:2.25 plus base entering the system through another syringe pump (middle); Heck coupling is performed in a packed bed reactor with Pd-SCM catalyst at 145 °C and 0.2 mL/min flowrate*

3.3.1 Continuous Tandem Synthesis of Hydroxystilbene **4**

In Figure 12, the results of the tandem experiment for the synthesis of hydroxystilbene **4** are plotted. As this product already served as a model compound in batch experiments, it was again used to demonstrate the long-term stability of the process. Therefore, this experiment ran for 300 minutes in contrast to 120 minutes for the synthesis of compounds **6** and **8**. These processes are believed to behave similarly in terms of production stability due to the high structural similarity of the target molecules.

After the startup phase of 60 minutes, almost constant product formation and yield could be observed with a slight increase at longer reaction times. A maximum yield of 56.9 % at 160 minutes and an average yield of 54.5 % over 60 minutes was obtained. Compared to the previous work of Gavric⁴ and Grabner³, the yield of the process could be more than doubled. During the startup phase, the conversion of vinylphenol **2** slightly decreased but then remained constant over time (above 75 %). While the ratio of hydroxystilbene **4** to side product **4b** did not change in the course of the experiment, the concentration of homoproduct **4a** decreased. This decline and the constant conversion indicate that no substantial catalyst degradation took place.

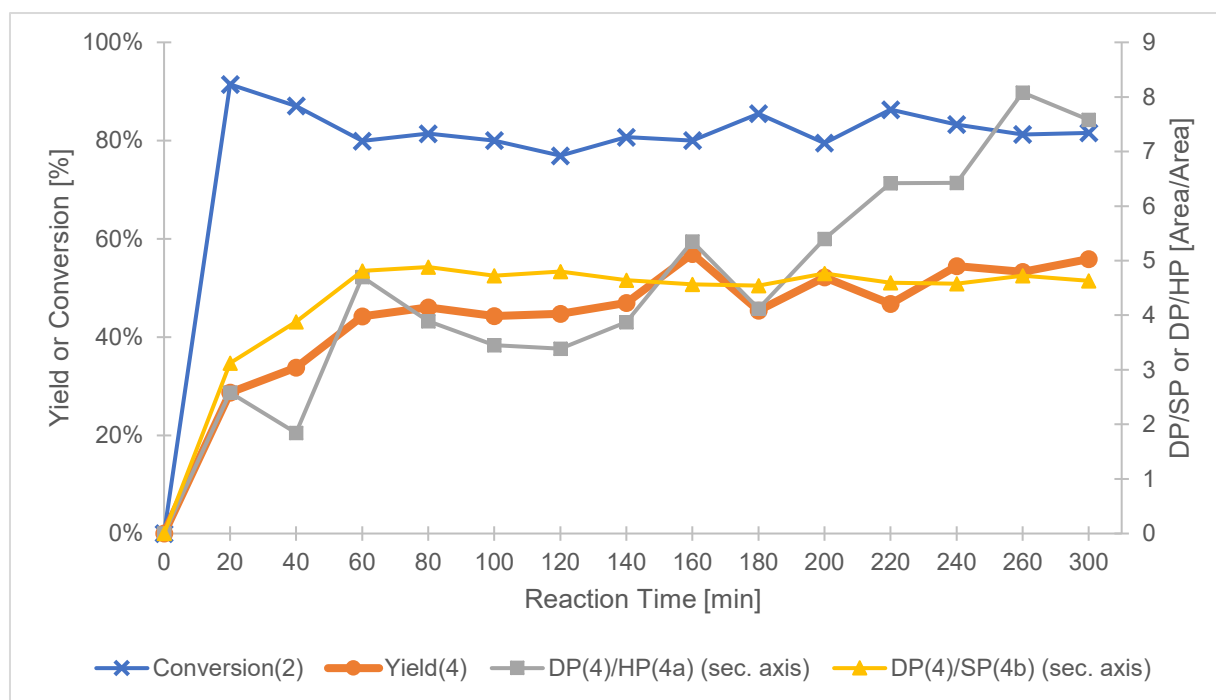


Figure 12 Tandem flow experiment results; conversion (blue), yield (orange), desired product **4** to homocoupling product **4a** peak area ratio (grey, sec. axis) and , desired product **4** to side product **4b** peak area ratio (yellow, sec. axis); experiments conducted according to chapter 4.4.2

3.3.2 Continuous Tandem Synthesis of Resveratrol **6**

In Figure 13 the results of the tandem experiment for the synthesis of resveratrol **6** are visualized. Over the whole analyzed reaction time, conversion, yield and homoproduction remained constant. The maximum yield achieved was 32.7 % after 40 minutes, whereas the average yield over 60 minutes was 32.1 %. Even if the yield of **6** was lower than the one of the hydroxystilbene **4** process using the same setup, the conversion of vinylphenol **2** was higher for all samples (>91 %). Additionally, less homoproduction **6a** was formed and DP/HP was determined to be >5.3 in contrast to values around 4 for **4a**. However, due to the missing calibration of the homoproduction **6a**, only the HPLC peak areas could be used to compare the extent of homoproduction formation in the different experiments. Thus, differences in the absorption coefficient could cause some errors and results should be considered as rough estimations.

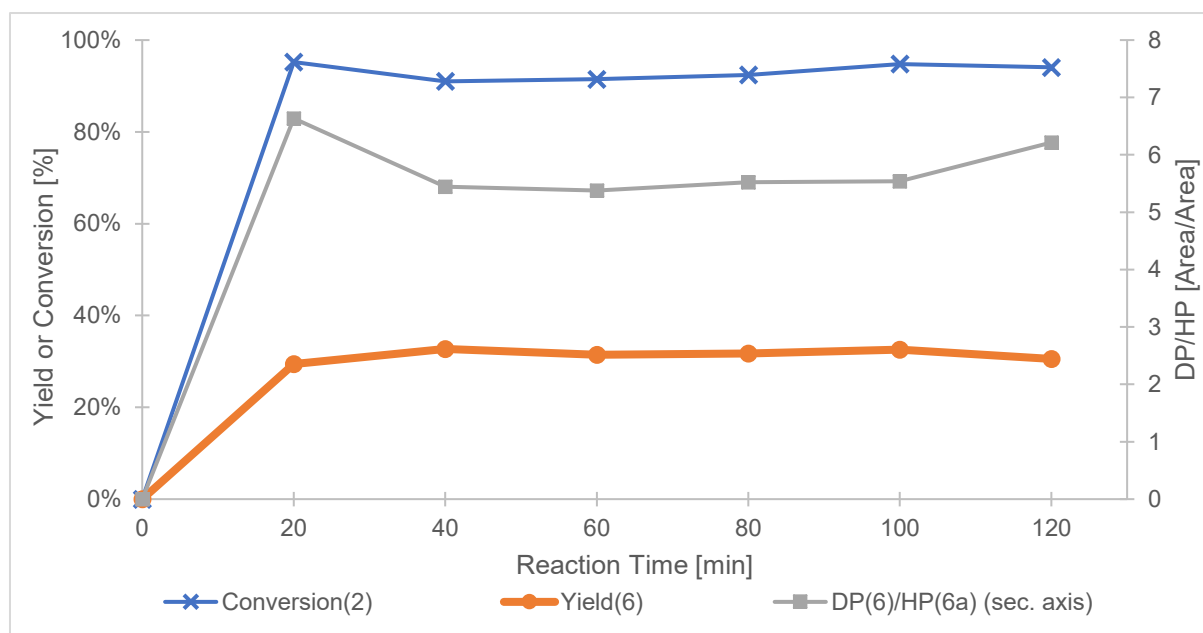


Figure 13 Tandem flow experiment results; conversion (blue), yield (orange), desired product **6** to homocoupling product **6a** peak area ratio (grey, sec. axis); experiments conducted according to chapter 4.4.2

3.3.3 Continuous Tandem Synthesis of Pterostilbene **8**

In Figure 14 the results of the tandem experiment for the synthesis of pterostilbene **8** are depicted. Yield, conversion and homoprodut formation were relatively constant over time, except from one sample after 40 minutes, which showed an exceptional yield of 62.3% as well as the highest extent of homoprodut formation. This could probably be caused by a measurement error as determined conversion and vinylphenol **2** concentration were similar to the other samples. A more reliable value for comparison with previous experiments is the average yield over 60 minutes with 50.1 %, which is lower than for hydroxystilbene **4** but significantly better than for resveratrol **6**. However, compared to the other experiments, in this process the highest amount of homoprodut **8a** was produced. As **8a** could be isolated and characterized via NMR and HPLC, a calibration could be performed and a 32 % higher homoprodut **8a** concentration compared to **4a** was determined. The conversion over the total reaction time was measured to be about 75-80 % and therefore in the same range as for the hydroxystilbene **4** synthesis. For HPLC calibration, in-house synthesized pterostilbene **8** and homoprodut **8a** were used. As the absolute purity for these substances was unknown, a purity of 95 % was estimated according to HPLC analysis as well as NMR measurements, causing a measurement uncertainty.

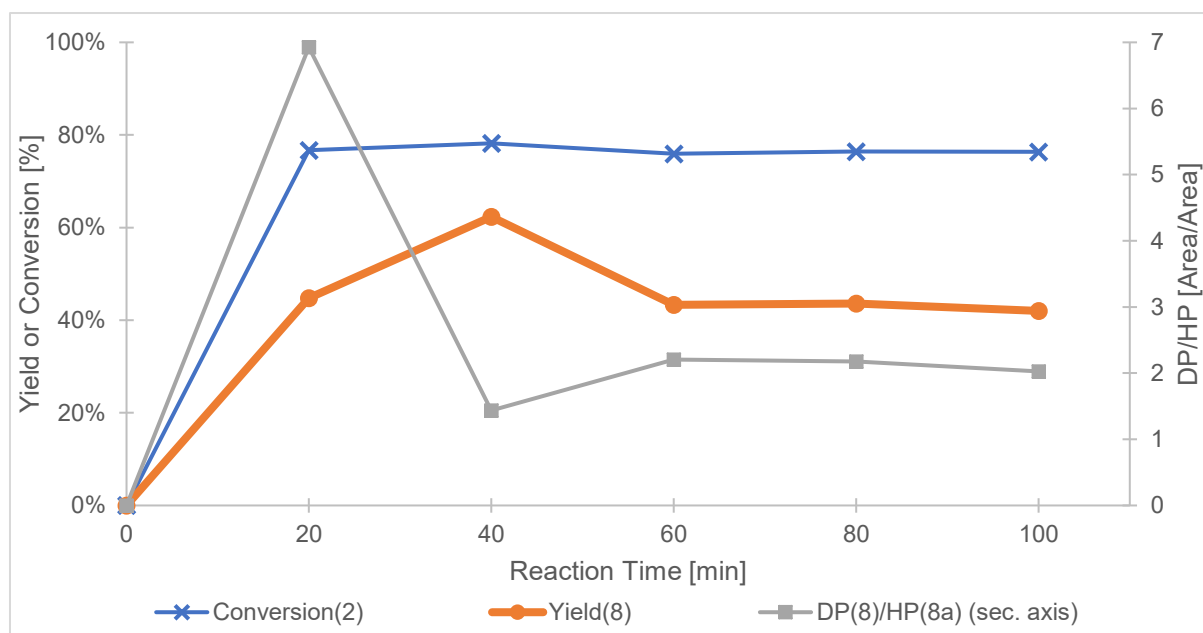


Figure 14 Tandem flow experiment results; conversion (blue), yield (orange), desired product **8** to homocoupling product **8a** peak area ratio (grey, sec. axis); experiments conducted according to chapter 4.4.2

3.4 Evaluation of Downstream Possibilities

Equally or even more important than the actual synthesis of an API are its isolation and purification. In this thesis, purification of the continuously synthesized products was always performed by liquid-liquid extraction followed by a column chromatography step. However, chromatographic processes are technically and economically unfavored for industrial scale production. One promising alternative to obtain the pure target compound is extraction followed by crystallization.

As the solvent mixture of the product stream (DES:Buffer(KPi):EtOH:H₂O = 6:5:6.75:2.25) contains more than 33 vol.% ethanol, the influence of this highly miscible solvent on extraction processes is critical for the design of an appropriate downstream process. Therefore, the effect of ethanol on the partition coefficient of resveratrol **6** between an organic phase (ethyl acetate) and the solvent mixture (aqueous phase) was determined experimentally and is depicted in Figure 15. With increasing volume fractions of ethanol, the partition coefficient decreases and shows an almost linear behavior. Consequently, the reduction of ethanol in the solvent mixture or the complete removal before the extraction improves the separation efficiency significantly. However, experiments using an ethanol-free solvent mixture (DES:KPi:H₂O = 6:5:9) result in a yield reduced by 6 % compared to the standard solvent mixture (DES:KPi:H₂O:EtOH = 6:5:2.25:6.75) under equal continuous flow conditions. Therefore, at least small amounts of ethanol are required in the solvent mixture to obtain sufficient yield and overcome solubility issues.

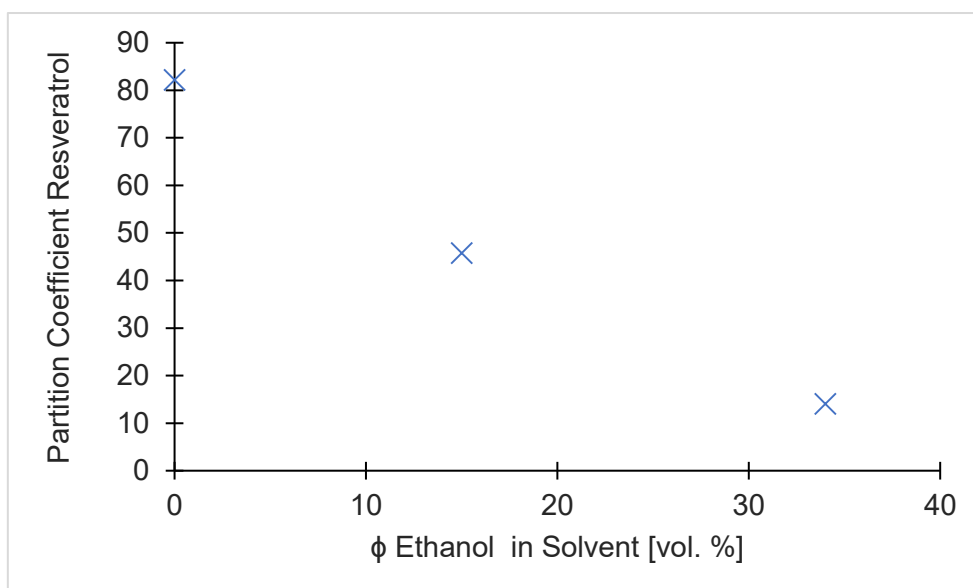


Figure 15 Partition coefficient of resveratrol; aqueous phase: solvent mixture [DES (30 %):KPi (25 %):H₂O (45- ϕ %):EtOH (ϕ %)] (vol.%; organic phase: ethyl acetate; 1:1 (v/v) mixture single stage in equilibrium

After the extraction process, crystallization of resveratrol **6** dissolved in ethyl acetate could be achieved by addition of a highly hydrophobic antisolvent like cyclohexane. However, residual amounts of DES were detrimental for this process as another phase formed. For the less polar product pterostilbene **8**, no crystallization experiments were carried out but polar antisolvents should be chosen due to the high solubility of the compound in cyclohexane.

3.5 Catalyst Leaching Experiments and Palladium Swing Catalysis

In this thesis, catalyst leaching and deactivation were major issues in terms of achieving high yields as well as a stable production process. It turned out that high temperatures increase the yield significantly but also promote catalyst leaching. Therefore, a compromise between these two aspects needed to be found and simply changing the type of Pd catalyst does not solve the problem. As described by Cantillo et al. and others, heterogeneous palladium catalysts are believed to involve a homogenous palladium species in the catalytic cycle, thus being prone to leaching and chromatographing of the active species from the solid support.^{28, 36, 37} To prevent the loss of palladium during the tandem process for the synthesis of stilbenes, a technical solution was required.

Therefore, the concept of palladium swing catalysis was developed in this thesis and could be used to minimize leaching, as can be seen in Figure 16. The idea was to place packed bed columns, filled with the SCM-palladium catalyst lacking palladium, at the beginning as well as at the end of the catalytically active zone for recovery purposes. In this way, palladium species leached from the catalytically active zone should be re-adsorbed, similar to described redeposition on the solid matrix in batch. Therefore, leaching is delayed, and the active catalytic species is slowly pushed towards the end of the packed bed. Before reaching the end of the column, the flow direction needs to be reversed and the active material is pushed towards the initial front of the column again. By alternating the flow direction after certain time intervals, the active species could be trapped inside the system.

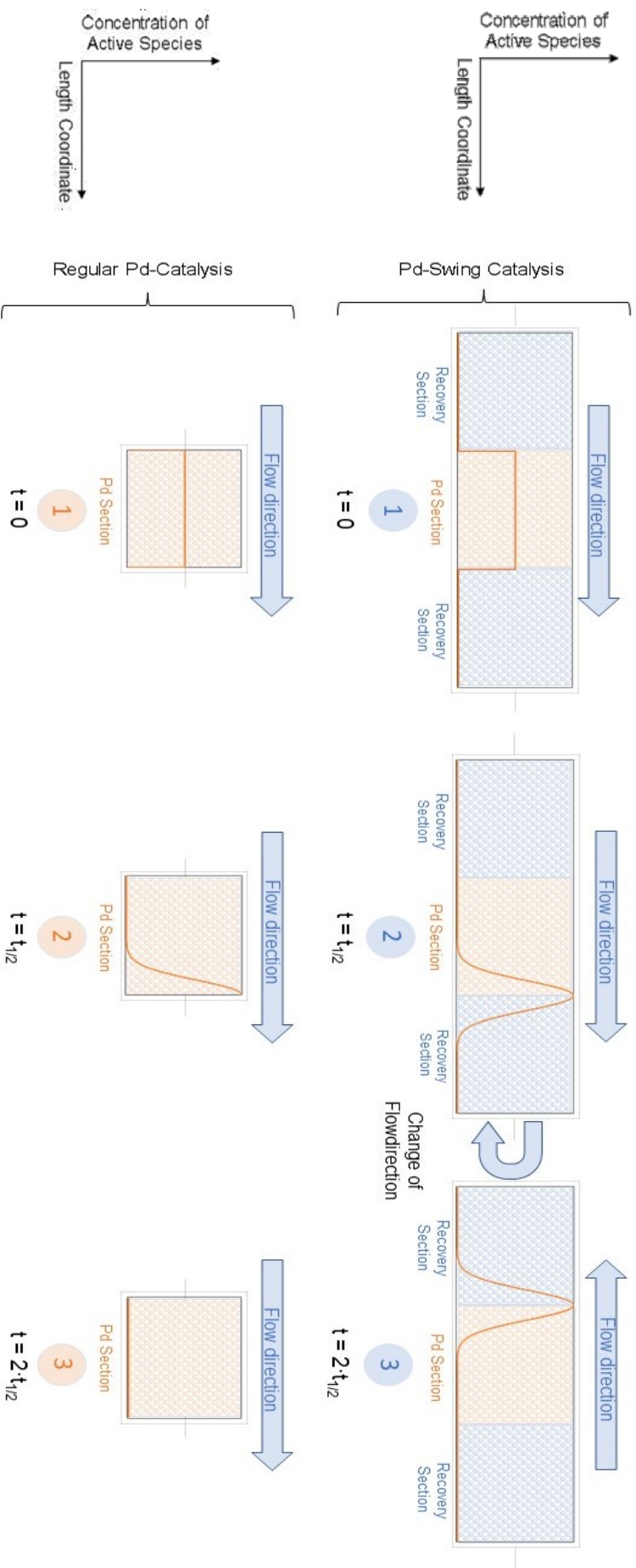


Figure 16 Concept of "Palladium Swing Catalysis", First row shows active species concentration profile for the Pd-swing catalysis: 1 $t = 0$ starting point, 2 $t = t_{1/2}$ half of the active species is pushed out of the Pd-section ($t_{1/2}$)-change of flow direction, 3 $t = 2 \cdot t_{1/2}$ the active species is pushed to the former front section of the Pd-section - the total system is still catalytically active; Second row shows regular case: 1 $t = 0$ starting point, 2 $t = t_{1/2}$ half of the active species is pushed out of the system, 3 $t = 2 \cdot t_{1/2}$ all of the active species is pushed out of the system-system is not catalytically active anymore

To prove if this concept is practically feasible, two experiments were performed. First, the leaching behavior of the Pd-SCM catalyst was analyzed according to chapter 4.4.4.1. Therefore, a standard Heck flow experiment as described in chapter 3.2.1 for the synthesis of hydroxystilbene **4** was performed at 150 °C. After 120 minutes of reaction time, catalyst samples were taken from the front, middle and back of the column. Then, the flow direction was reversed and after another 120 minutes, samples were withdrawn from the same positions. With these catalyst samples, batch experiments similar to the ones summarized in chapter 3.1 were performed to determine the remaining catalyst activity. The results of these experiments as well as results from the flow experiment are plotted in Figure 17. As the catalyst was sampled wet, the average dry mass was determined to get comparable results for the activity. As predicted in the model, the active species was pushed towards the end of the column during the flow experiment and only the “Col. End 120 min” sample was shown to still be catalytically active (18 % yield, full conversion). Even though a higher yield could be achieved with this sample, the activity decreased compared to the fresh catalyst. After change of the flow direction, as expected the position of the active species was reversed. Only the front sample “Col. Front 240 min” showed product formation with a yield of 8 %. The concentration of biphenyl **4a**, which corresponds to the remained active species in the catalyst bed according to the findings described in chapter 3.2, increased from 0.65 mM at 120 minutes to 1.58 mM after 240 minutes of reaction time. Additionally, the lower conversion and yield after 240 min indicate that leaching had already taken place at this time. Hence, active material must have already been pushed out from the column, thus explaining the lower activity, yield and conversion of the “Col Front 240 min” sample. Shorter time intervals between the change of flow direction could help to minimize this loss. In general, the samples withdrawn during the flow experiments showed higher yields. However, considering the massive amount of catalyst used, the specific activity is low.

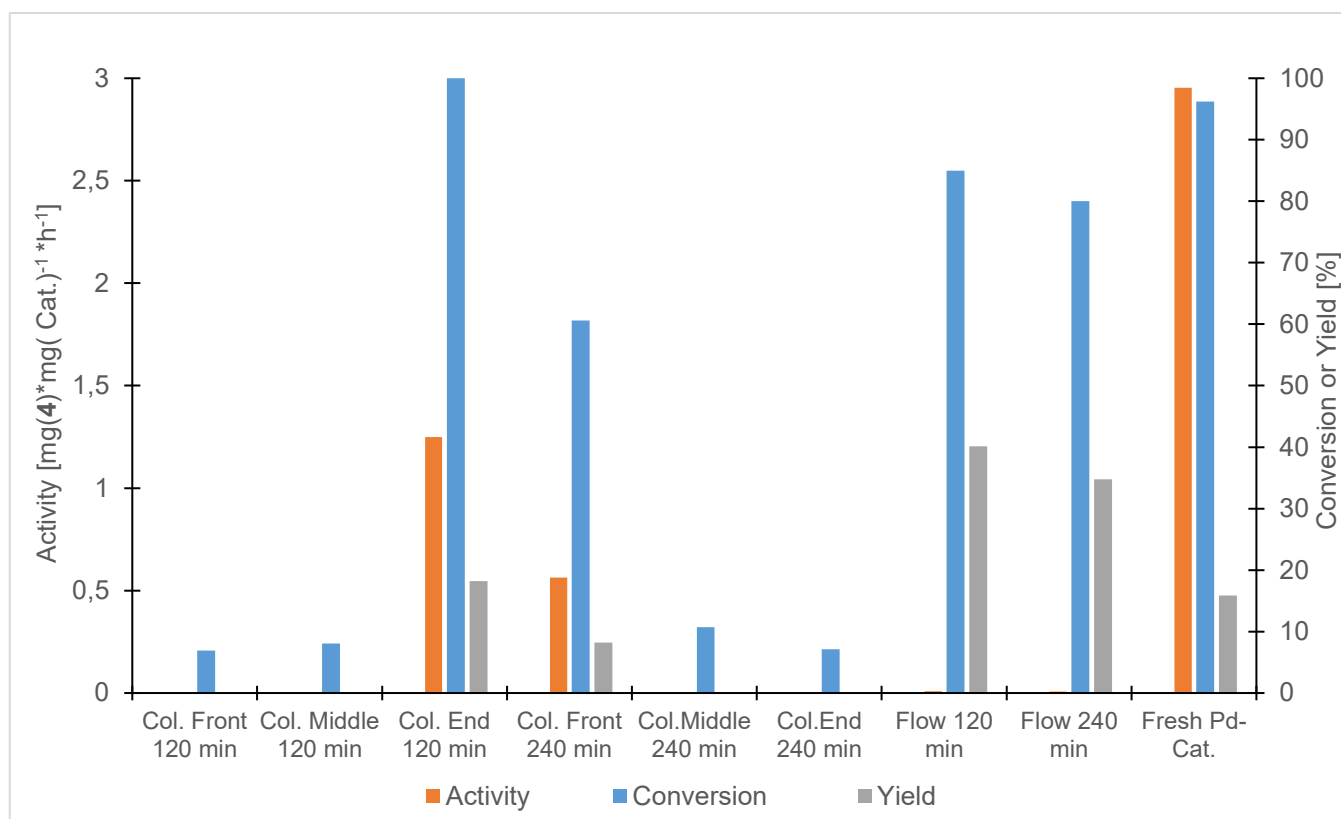


Figure 17 Activity, conversion (2) and yield (4) of different column positions in a palladium swing catalysis setup without recovery sections, flow direction change after 120 minutes, according to procedure 4.4.4

The second catalyst leaching experiment was performed to evaluate the feasibility of the recovery section. Therefore, a standard Heck flow experiment comprising a second column filled with recovery SCM material, installed directly after the Pd-SCM catalyst column, was performed according to 4.4.4.2. After 240 minutes of reaction time and intensive flushing with solvent, catalyst samples were withdrawn from different positions of the catalytic as well as recovery column. The catalyst samples were again analyzed in batch experiments and obtained results are visualized in Figure 18. The active Pd species was pushed to the end of the column, represented by the “Pd-Column Back” sample with a determined yield of 15.5 %. Interestingly, the “Pd-column Front” sample showed very little activity and yield, which might be explained by dead zones at the screw cap. In the recovery column, active catalytic species was found in the middle of the packed bed, giving a yield of 10.5 %. This result can be explained by the intensive flushing of the column with solvent after the reaction. The active species located at the front of the recovery column was pushed to the middle due flushing with more than 5 times the column volume at elevated temperature. Furthermore, the excellent yield of 70.5 % determined from a sample withdrawn during the flow experiment is worth mentioning. It might be explained by the high reaction temperature and a very active catalyst.

In all experiments using the SCM catalyst, it could be qualitatively observed that leaching and activity is related to the particle size of the catalyst powder. Small particles that were grinded intensively during preparation tend to leach faster but show better activity. Consequently, for the leaching experiments a very fine powder was used, explaining the outstanding yield of 70.5 % during the flow experiment as well as the fast leaching. For the tandem experiments, a more coarse powder was used to achieve stable product formation for more than 300 minutes.

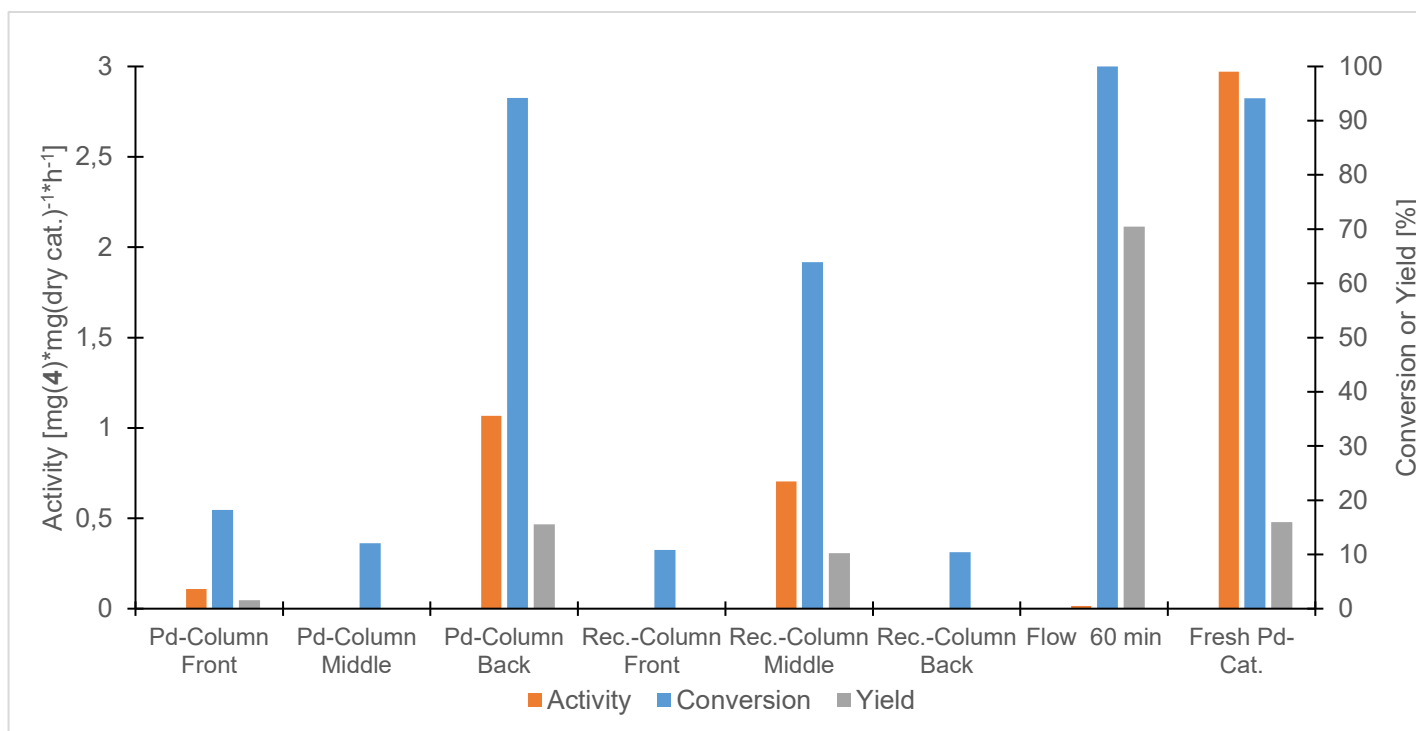


Figure 18 Activity, conversion (2) , yield (4) of different column positions, Pd-column followed by a recovery column without change of flow direction, both columns washed with 10 times the column volume

4 Experimental

4.1 Equipment

4.1.1 Flow Equipment

4.1.1.1 Pumps

Syringe pumps: LAMBDA[®] VIT-FIT HP - microprocessor-controlled programmable syringe pump. Used with 20 mL stainless steel syringes.

HPLC pump: P4.1S (Knauer; AZURA[®] Compact; max. flow rate: 10 mL/min).

4.1.1.2 Packed bed reactors

Empty preparative stainless steel HPLC columns were used as packed bed reactors. Depending on their use for the enzymatic decarboxylation or the Heck reaction, they were filled with enzyme beads or palladium catalyst powder and compressed by shaking and vibrations. To prevent leaching of solids and leaking, a paper filter, metal filter, sealing ring, sealing cap and column cap were used on each side. Different column sizes were used (L x I.D. 120 x 8 mm for decarboxylation reactions, L x I.D. 40 x 8 mm for Heck reactions).

4.1.1.3 Fittings and Capillaries

The used capillaries, fittings and syringe adapters were standard HPLC equipment. Inner diameter of capillaries: 0.03 inch (0.762 mm).

4.1.1.4 Back pressure regulator

BPR Cartridge 75 psi (5.17 bar) Gold Coat P-762 (IDEX Health & Science).

4.1.2 Batch Equipment

4.1.2.1 Batch Setup for the Simultaneous Performance of Multiple Heck Couplings

To perform up to eight batch Heck couplings at a time, a metal plate with eight circularly arranged holes was placed over an oil-bath equipped with a magnetic stir bar. In the holes, 10 mL vials from the Crystalline[®] apparatus were placed including a magnetic stir bar and closed with a screwable septum cap. To maintain atmospheric pressure inside the vials and for syringe sampling, cannulas were placed on top. For temperature control and stirring, a magnetic stirrer equipped with a temperature control unit was used (Figure 19).



Figure 19 Multiple batch setup for Heck couplings (in the heat up phase)

4.2 Analytics

4.2.1 High Performance Liquid Chromatography

HPLC Unit: Agilent 1100 series HPLC system equipped with online degasser, quaternary pump, autosampler, thermostated column compartment and UV-VIS diode array detector.

Column: ThermoFisher Scientific Accucore™ C18 reversed phase column (50 x 4.6 mm ID; 2.6 μm).

Method: See Table 4; flow rate: 1 mL/min, column temperature 25 °C, 2.0 μL injection volume.

Eluents: Buffer H₂O:H₃PO₄ = 300:1 (v/v), Methanol HPLC grade.

Calibration taken from Gravic (**4**, **4a**, **4b**) and done with commercially available pure substances (**1**, **2**, **3**, **6**) as well as self-synthesized substances (**5**, **7**, **8**, **8a**)

Table 4 HPLC methods, methanol and buffer (H₂O:H₃PO₄ 300:1) gradients

Method	MeOH [v/v]	Buffer [v/v]	Gradient [min]	Run Time [min]	Flow Rate [mL/min]
A	40	60	1	16	1
	90	10	12		
	40	60	14		
B	20	80	1	20	1
	30	70	8		
	60	40	12		
	60	40	17		
	30	70	20		

Method A was used for experiments synthesizing hydroxystilbene and pterostilbene, method B for resveratrol.

Table 5 Retention time and detector wavelength for analyzed compounds

Compound	Method	Time [min]	Wavelength [nm]
<i>para</i> -coumaric acid 1	A	1.1	282
	B	1.8	282
4-vinylphenol 2	A	3.2	237
	B	9.1	237
iodobenzene 3	A	7.9	237
4-hydroxystilbene 4	A	8.3	237
biphenyl 4a	A	8.5	282
<i>para</i> -hydroxy-1,1-diphenylethylene 4b	A	9.8	252
2,4-dihydroxyiodobenzene 5	B	6.4	237
resveratrol 6	B	7.5	310
[1,1'-biphenyl]-3,3',5,5'-tetraol 6a	B	0.7	237
2,4-dimethoxyiodobenzene 7	A	8.6	237
pterostilbene 8	A	7.9	282
3,3',5,5'-tetramethoxy-1,1'-biphenyl 8a	A	9.1	282

4.2.2 pH-Meter

Electrode: Mettler Toledo InLab ® Expert Pro-ISM 0-14 pH.

Calibration was done weekly with pH 4.0, 7.0 and 10.0 buffers from Mettler Toledo LTD.

4.2.3 Flow-through UV-Vis Spectrometry

Source Avantes AvaLight-DS, Spectrometer vAvaSpec-ULS2048.

4.2.4 Thin Layer Chromatography

For thin layer chromatography, TLC plates from Merck (Silica gel 60 F₂₅₄ aluminum sheets, 20x20 cm) were used. For detection UV-light (254 nm) was used.

4.3 Batch Experiments and Synthesis

4.3.1 Deep Eutectic Solvent Preparation

For the deep eutectic solvent used in this work, choline chloride (ChCl) served as quaternary ammonium salt and glycerol as hydrogen bond donor and liquid. For its preparation, a mixture of the two components in a molar ratio of ChCl:Glycerol = 1:2 (mol/mol) was heavily stirred and heated to 80°C in a 500 mL Erlenmeyer flask. After cooling down slowly to room temperature, a clear viscous colorless liquid was obtained, which stayed clear over time and could be stored at room temperature (RT) until usage.

4.3.2 Potassium Phosphate Buffer (KPi-Buffer) Preparation

To ensure optimal enzyme performance, a KPi-Buffer was used as reaction medium for decarboxylation reactions. For the preparation of the buffer, KH₂PO₄ (2.99 g, 21.97 mmol) and K₂HPO₄ (0.53 g, 3.04 mmol) were dissolved in 500 mL deionized water, resulting in the required pH 6.0.

4.3.3 Synthesis of Palladium Solution Combustion Catalyst Ce_{0.2}Sn_{0.79}Pd_{0.01}O_{2-δ}

In order to prepare the heterogeneous palladium catalyst, the solution combustion method reported by Baidya et al. and modified by Lichtenegger et al. was used.^{29, 38} In a mortar ammonium cerium(IV) nitrate (6.370 g, 11.6 mmol), tin(II) oxalate (9.489 g, 45.9 mmol), glycine (10.038 g, 133 mmol) and palladium(II) chloride (0.102 g, 0.575 mmol) were pestled until a fine and homogeneous powder was obtained. After the addition of 6 ml deionized water the suspension was transferred into a 600 mL beaker and further homogenized in an ultrasonic bath for 30 minutes. The dark brown viscous suspension was heated to 350 °C in a muffle oven for combustion. The voluminous product was pestled in a mortar and the fine powder heated overnight at 350 °C. The product was obtained as a yellow powder in almost quantitative yield (~9 g).

4.3.4 Enzyme Immobilization for the Preparation of Alginate Beads

The enzyme *BsPAD* for decarboxylation was obtained as cell-free extract in form of a freeze-dried powder from the Institute of Molecular Biotechnology (TU Graz) and needed to be encapsulated prior to the use in a flow setup. To prepare the alginate beads, 80.0 mg cell-free extract and 40.0 mg sodium alginate were dissolved in 2 mL KPi-buffer. The yellowish viscous solution was added dropwise with syringe and canula to a 2 w% BaCl₂-solution under gentle stirring. In this way, beads of 1-3 mm diameter were formed and stirred for 1 h to further solidify. With a sieve, the beads were recovered from the solution and washed with 0.9 w% NaCl-solution. After drying on filter paper for 30 minutes under ambient conditions, they were ready for use.

4.3.5 General Procedure Heck Coupling Experiments

As described in 4.1.2.1, a special experimental setup was used to perform multiple Heck coupling batch experiments at the same time.

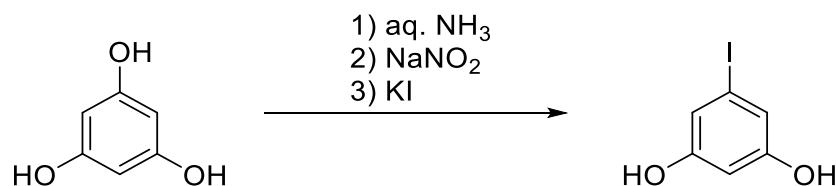
To get the appropriate solvent for the reactions, a mixture of DES:Buffer(KPi):H₂O:EtOH = 6:5:2.25:6.75 (v/v) was produced beforehand and was stored in capped bottles. Depending on the used base, the appropriate amount of potassium carbonate (0-10 mol eq.) was added and dissolved. For adjustment of the pH, 0.5 or 1 M KOH solution was added dropwise and pH was checked with the pH-meter. After transferring 6 mL of the viscous basic clear solvent mixture into the crystalline vials, vinylphenol **2** (1.00 mol eq.) and iodobenzene **3** (1.50 mol eq.) were added according to

. After closing the vial with septum caps and equipping them with cannulas, the substrates were dissolved by stirring and heated for 30 min at 80 °C in the oil bath. After taking a reference sample, the catalyst (1.9 mg) was quickly added and samples (100 µL) were withdrawn from the reaction solution after 10, 20 and 30 min. In a HPLC vial, 50 µL of the sampled reaction mixture were diluted with 500 µL MeOH:H₃PO₄=7:3 (v/v).

The HPLC analysis was done according to 4.2.1.

Table 6 List of: Substrates and K₂CO₃ concentrations as well as different pH-values used for batch Heck couplings

Conc. Vinylphenol 2 [mM]	Conc. Iodobenzene 3 [mM]	Conc. K ₂ CO ₃ [mM]	pH - Values
10	15	0	10.5
25	37.5	15	11
40	60	45	11.5
		100	12
			12.5
			13

4.3.6 Synthesis of 5-iodobenzene-1,3-diol **5**

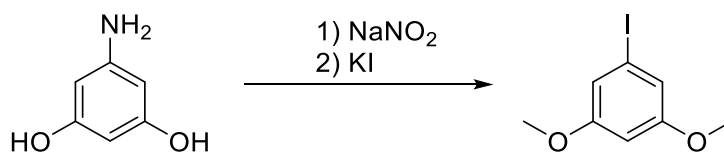
Scheme 4 Synthesis of 5-iodobenzene-1,3-diol 5, procedure from ³⁹

In a 250 mL round bottom flask, phloroglucinol (10.0 g, 79.3 mmol, 1.00 mol eq.) was dissolved over 30 minutes in ammonia solution (60 mL, 1.00 mol, 12.6 mol eq., 33 w%) at 0 °C. Afterwards, the pink suspension was stirred for 20 hours at RT. Under reduced pressure, the solvent was removed from the red brown solution and the received brown-red solid was dissolved in 5N aq. HCl solution (30 mL, 150 mmol, 1.90 mol eq.). The solvent was again removed under reduced pressure and a brown solid (28.11 g) was obtained. This intermediate product was dissolved in deionized ice-cold water (400 mL) and H₂SO₄ (18.9 mL, 340 mmol, 4.20 mol eq., 98 w%) was added over 5 minutes. After the slow addition of NaNO₂ (19.0 g, 275 mmol, 3.40 mol eq.) dissolved priorly in 78 ml deionized water, the suspension was stirred at 0 °C for 15 min. KI (58.5 g, 352 mmol, 4.50 mol eq.) dissolved in 60 mL deionized water was added dropwise under controlled nitrogen evolution. The formed red suspension was stirred for 5 h. TLC reaction monitoring (EtOAc:PE = 3:7) showed the formation of the diiodo product although the substrate was not fully converted. To minimize byproduct formation, the reaction was stopped by extracting the reaction mixture with EtOAc (3x 150 mL). Collected organic layers were washed with 25 w% K₂S₂O₃ (2x 100mL), 1 N HCl (3x 100 mL), brine (1x 100 mL) and were subsequently dried over Na₂SO₄. The solvent was removed under reduced pressure and 28.1 g of a brown oil was obtained. The crude product was purified by column chromatography (SiO₂, EtOAc:PE:Tol = 3:6:1, R_f = 0.6) giving the product as yellowish crystals in 24.8 % yield (4.66 g, 19.7 mmol).

¹H NMR (300 MHz, C₆D₆) δ [ppm] = 7.16 (s, 2H, O-H), 6.43 (s, 2H, Ar-H), 5.96 (s, Ar-H)

¹³C NMR (76 MHz, C₆D₆) δ [ppm] = 157.8 (C_{Ar}), 117.3 (C_{Ar}), 102.8 (C_{Ar}), 94.0 (C_{Ar})

4.3.7 Synthesis of 3,5-dimethoxy-1-iodobenzene 7



Scheme 5 Synthesis of 3,5-dimethoxy-1-iodobenzene 7, procedure from ⁴⁰

In a 100 mL round bottom flask, 3,5-dimethoxy-1-aniline (5.00 g, 32.6 mmol, 1.00 mol eq.) was suspended in hydrochloric acid (20 mL, 0.25 mol, 7.66 mol eq.) together with 20 g ice and external cooling to 0 °C. The slow addition of NaNO₂ (2.70g, 39 mmol, 1.20 mol eq.) over 20 minutes led to a black suspension which was stirred for 10 minutes. Solid KI (30.0 g, 1.80 mol, 50 mol eq.) was added under controlled nitrogen evolution and cooling to 0°C. The dark brown solution was stirred for 30 minutes at 0 °C and then 14 hours at RT. The reaction was stopped by extracting the reaction mixture with diethyl ether (3x 50 mL). Collected organic layers were washed with saturated Na₂SO₃ (2x 50mL) and brine (1x 50 mL) and were subsequently dried over Na₂SO₄. The solvent was removed under reduced pressure and 3.05 g of a brown solid were obtained. The crude product was purified by column chromatography (SiO₂, EtOAc:PE = 9:1 R_f = 0.65) giving the product as colorless crystals with a characteristic smell in 22.6 % yield (1.95 g, 7.38 mmol)

¹H NMR (300 MHz, CDCl₃) δ [ppm] = 6.89 (s, 2H, Ar-H), 6.44 (s, 1H, Ar-H), 3.79 (s, 6H, CH₃)

¹³C NMR (76 MHz, CDCl₃) δ = [ppm] 161.1 (C_{Ar}), 115.8 (C_{Ar}), 100.7 (C_{Ar}), 94.1 (C_{Ar}), 55.5 (CH₃)

4.4 Continuous Experiments

4.4.1 Single Step Heck Coupling Flow Experiments

Different experiments were conducted with various iodoaryl substrates as well as changing experimental properties and listed in Table 7. However, the general procedure is similar for all different runs. The general setup, which was used for all experiments, is shown Scheme 2. As syringe pump, a Lambda VIT-FIT HP pump with a flow rate of 0.205 or 0.410 mL/min equipped with a 20 mL stainless steel syringe was used. As solvent, a mixture of DES:Buffer (KPi):H₂O:EtOH = 6:5:2.25:6.75 (v/v) was used. After the addition of 15 mM K₂CO₃, the pH-value was set to 11.75 by adding 50 w% KOH dropwise by means of a pH-meter. An empty HPLC column filled with Pd-SCM catalyst was used as packed catalyst bed with ~ 1.6 g (10 mmol, 1 mol% Pd) catalyst. Substrates were added to this basic solution according to Table 7. Before the reaction solution was pumped through the system, the setup was flushed with the solvent mixture for a minimum of 30 min with the same volumetric flow as in the following

experiment. Palladium black formation could be observed at the beginning of the experiments in the heat up phase. To maintain an elevated pressure of 5.2 bar, a backpressure regulator was used. Samples were taken periodically analog to the batch experiments.

Table 7 Experiment parameters and analyzed parameters of continuous Heck coupling reactions

Entry	Educts	Temperatures [°C]	Flow rates [mL/min]	Purpose/Analyzed Parameter
1	10 mM 2 15mM 3	80,90,100,110	0.1	Pd-leaching for ICP-MS, temperature
2	20 mM 2 30 mM 5	130, 160	0.2, 0.4	resveratrol production, flow rate
3	10 mM 2 15 mM 3	140,160,170,180,200	0.2	temperature
4	10 mM 2 15 mM 5	140,150,160	0.2	cat. stability
5	20 mM 2 30 mM 7	120,140,160	0.2	pterostilbene production temperature, cat. stability

Using the described continuous setup, resveratrol **6** could be synthesized (Table 7, Entry 2) in 21.9 % yield over 60 min. For isolation of the target compound, ethanol was removed from the collected outlet flow under reduced pressure and the dark red solution was extracted with EtOAc (3x 50 mL) and dried over Na₂SO₄. The crude product was purified by column chromatography (SiO₂, EtOAc:Toluene = 3:7, R_f = 0.45 in EtOAc:CH = 6:4) giving the product as colorless crystals.

¹H NMR (300 MHz, DMSO) δ [ppm] = 9.37 (s, 1H, O-H), 9.01 (s, 2H, O-H), 7.22 (d, J = 8.3 Hz, 2H, Ar-H), 6.76 (d, J = 16.4 Hz, 1H, C=C-H), 6.66 (d, J = 16.4 Hz, 1H, C=C-H), 6.58 (d, J = 8.3 Hz, 2H, Ar-H), 6.21 (s, 2H, Ar-H), 5.94 (s, 1H, Ar-H).

¹³C NMR (76 MHz, DMSO) δ [ppm] = 158.5 (C_{Ar}), 157.2 (C_{Ar}), 139.2 (C_{Ar}), 128.1 (C_{Ar}), 127.8 (C_{Ar}), 125.6 (CH), 115.5 (C_{Ar}), 104.3 (C_{Ar}), 101.7 (C_{Ar}).

Utilizing the same experimental setup, pterostilbene **8** could be synthesized as well in continuous flow in 48.2 % yield (Table 7, Entry 5). After extraction from the collected outlet flow, the crude product was purified by column chromatography (SiO₂, EtOAc:CH = 2:8, R_f = 0.50 in EtOAc:CH = 3:7) giving the product as colorless crystals.

^1H NMR (300 MHz, CDCl_3) δ [ppm] = 9.79 (s, 1H, O-H), 7.32 (d, J = 8.5 Hz, 2H, Ar-H), 6.95 (d, J = 16.2 Hz, 1H, C=C-H), 6.81 (d, J = 16.3 Hz, 1H, C=C-H), 6.75 (d, J = 8.5 Hz, 2H, Ar-H), 6.57 (s, 2H, Ar-H), 6.31 (s, 1H, Ar-H), 3.75 (s, 6H, CH_3).

^{13}C NMR (76 MHz, CDCl_3) δ [ppm] = 161.0 (C_{Ar}), 155.4 (C_{Ar}), 139.7 (C_{Ar}), 130.2 (C_{Ar}), 128.7 (CH), 128.0 (C_{Ar}), 126.7 (CH), 115.7 (C_{Ar}), 104.4 (C_{Ar}), 99.7 (C_{Ar}), 55.4 (CH_3).

The homocoupling side product 3,3',5,5'-tetramethoxy-1,1'-biphenyl **8a** could be isolated as well by column chromatography using abovementioned conditions and was characterized by NMR.

^1H NMR (300 MHz, CDCl_3) δ [ppm] = 6.64 (s, 4H), 6.40 (s, 2H), 3.77 (s, 12H).

^{13}C NMR (76 MHz, CDCl_3) δ [ppm] = 161.0(C_{Ar}), 143.5(C_{Ar}), 105.6(C_{Ar}), 99.5(C_{Ar}), 55.5(CH_3).

4.4.2 Chemo Enzymatic Tandem Flow Experiments

The general flow scheme of performed experiments is depicted in Scheme 3 Tandem flow experiment comprising enzymatic decarboxylation as well as Heck coupling of vinylphenol with various iodoaryl substrate to give stilbenes and a picture of the tandem flow experiment is shown in Figure 20. The first syringe pump was used to pump coumaric acid **1** (20.0 mM, 1.00 mol eq.), dissolved in DES:KPi = 1:1, through the decarboxylation column (L x I.D. 8 x 120 mm) with a flow rate of 0.1 or 0.2 mL/min. Used HPLC column was filled with enzyme beads containing 160 mg BsPAD enzyme, immobilized according to 4.3.4, and was heated to 30 °C using a water bath. In this way, the intermediate compound vinylphenol **2** could be produced enzymatically in almost quantitative yield. Then, the product stream was mixed using a T-mixer with either iodobenzene **3**, dihydroxyiodobenzene **5** or dimethoxyiodobenzene **7** (30.0 mM, 1.50 mol eq.) dissolved in DES:EtOH:H₂O = 1:6.75:2.25 containing also K₂CO₃ (30.0 mM, 1.50 mol eq.) as well as KOH (43.7 mM, 2.18 mol eq.). The second syringe pump was operated with the same flow rate as the first one to get a total flow rate of 0.2 or 0.4 mL/min, respectively. The Heck coupling part of the tandem setup was prepared and used analog to 4.4.1 and used at temperatures between 145 and 160 °C.

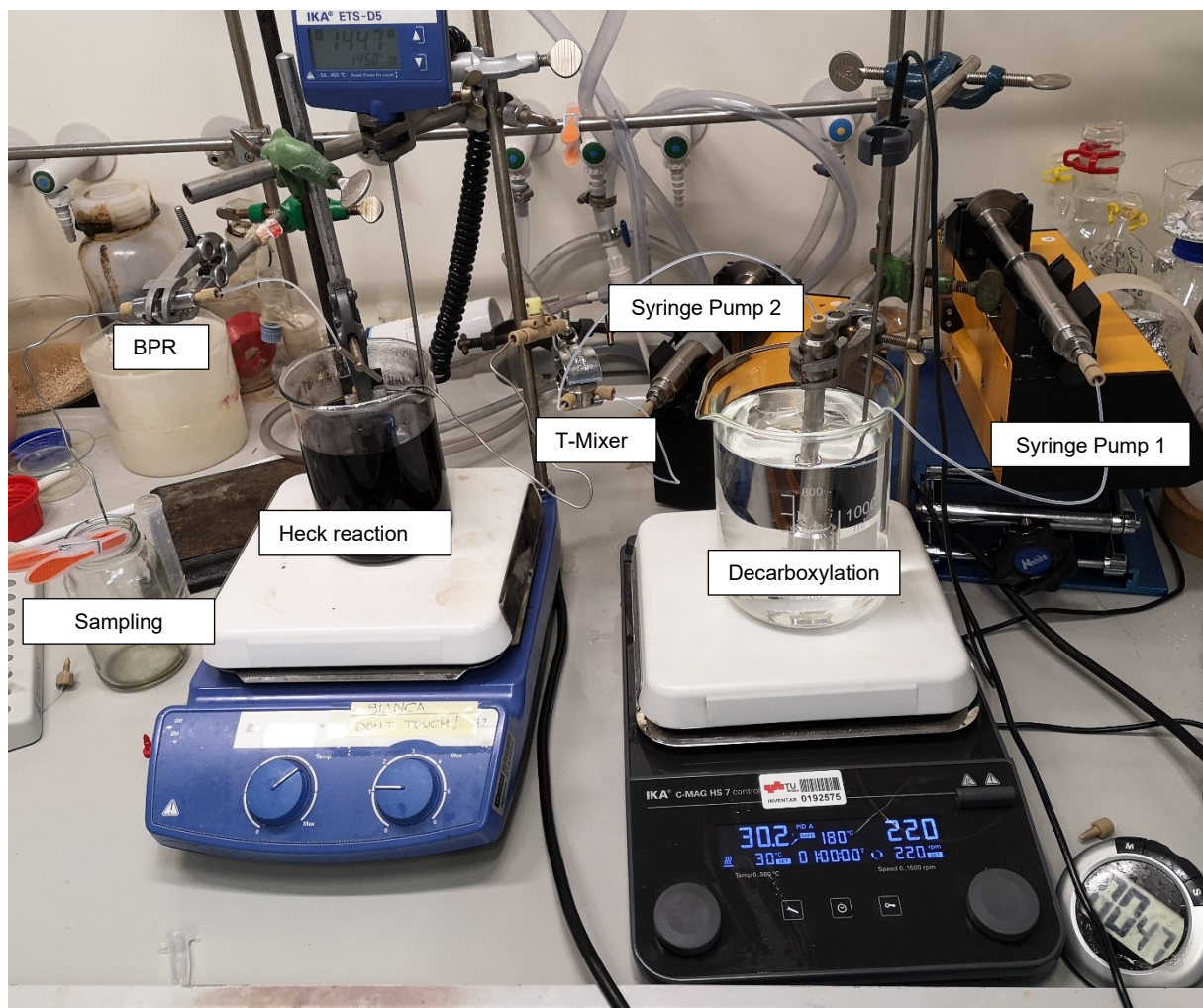


Figure 20 Chemo enzymatic tandem setup

4.4.3 Residence Time Distribution Measurements

To characterize the used flow setups, the residence time distribution of the enzyme reactor, the Heck coupling reactor, the combined tandem setup and the tubing alone without reactors was measured via inline UV-Vis measurement of the tracer anisole.

As tracer, an anisole solution (0.008 v% anisole in 12 w% ethanol in water) was used. This tracer could be detected by using a flow cell with 1 cm pathlength and an Avantes® UV-Vis detector. While the tracer signal was measured after the reactor at wavelengths between 268-274 nm, the background noise was measured simultaneously at 500-506 nm with a frequency of one datapoint per second.

The flow setups were assembled exactly as in the experiments described in 4.4.1 and 4.4.2 and filled with SCM-catalyst and enzyme beads (without active enzyme). To enable a sharp signal and a quick change between the solvent for flushing and the tracer solution, a manual 6-way valve was used. Before every measurement, the system was flushed for approximately

45 minutes until a steady signal was obtained. The used syringe pumps and flow rates are summarized in Table 8, whereas results are apparent from Table 9. Results are calculated according to Equation 1 for the mean residence time and according to Equation 2 for the Bodenstein number. The closed-closed dispersion model was used as the flow regime coming from the capillaries changed significantly after entering the reactor.

Table 8 Pump setup for residence time distribution measurements

Pump	Setting	Flow rate [mL/min]	Use	Regular Use
Lambda 1	5	0.114	Solvent for mixing	Coumaric acid
Lambda 2	18	0.102	Tracer	Reaction solution
Lambda 3	5	0.115	Solvent flushing	/

Equation 1 Mean residence time \bar{t}

$$\bar{t} = \frac{1}{c(\max)} * \sum t_i * \Delta c_i$$

Equation 2 Bodenstein-number for a closed-closed vessel model

$$Bo_{cc} = \left(\frac{1}{\sigma_{\theta}^2} - 1 \right) + \sqrt{\left(\frac{1}{\sigma_{\theta}^2} - 1 \right)^2 + \left(\frac{2}{\sigma_{\theta}^2} - 2 \right)} \quad \text{with} \quad \sigma_{\theta}^2 = \frac{\sum t_i^2 * c_i * \Delta t_i - \bar{t}^2}{\sum c_i * \Delta t_i}$$

Table 9 Results residence time distribution measurements

Reactor	Mean residence time \bar{t} [min]	Bodenstein Number Closed-Closed
Piping	6.7	17.9
Heck Reactor	13.6	50.1
Tandem Set-up	38.5	12.1

4.4.4 Leaching experiments

4.4.4.1 Pd-SCM Catalyst Column Leaching Experiment

A continuous Heck coupling experiment according to chapter 4.4.1 was performed using 10 mM vinylphenol **2**, 15 mM iodobenzene **3**, 15 mM K₂CO₃ and 22 mM KOH at 150 °C and a flow rate of 0.2 mL/min. After 120 minutes reaction time, a flow sample was taken and the experiment was stopped to take samples of the catalyst (~15 mg) from the front, middle and back of the column. The column was screwed again upside down into the setup to reverse the flow direction. After another 120 minutes of reaction time the column was flushed with 10 mL solvent and catalyst samples were withdrawn again from the same positions.

With these catalyst samples batch experiments according to chapter 4.3.5 were performed using 10 mg of the wet catalyst, 10 mM vinylphenol **2**, 15 mM iodobenzene **3**, 15 mM K₂CO₃ and 22 mM KOH. Sampling was done after 20 minutes. To calculate the specific activity the dry mass of the wet catalyst samples was analyzed by drying roughly 100 mg of wet catalyst for 24 hours at 300 °C.

Equation 3 specific activity

$$\text{specific activity} = \frac{\text{concentration}(4) * \text{molar mass}(4) * \text{volume}}{\text{mass}(\text{dry catalyst}) * \text{reaction time}}$$

4.4.4.2 Pd-SCM Catalyst and Recovery Column Leaching Experiment

First, the Pd free catalyst powder for the recovery column was prepared by synthesizing the SCM catalyst according to chapter 4.3.3 but without adding palladium(II) chloride.

The experiment was performed similarly as described in chapter 4.4.4.1. However, after the regular Pd-SCM column another equal-sized HPLC column packed with Pd free catalyst was attached as recovery column. The experiment was run for 240 minutes without any flow direction change. The columns were flushed separately with 10 mL solvent. Samples from the front, middle and back of both columns were withdrawn and analyzed in batch experiments according to chapter 4.4.4.1.

5 Conclusion and Outlook

In previous works⁴, hydroxystilbene **4** has been synthesized in a continuous chemo-enzymatic tandem process in yields of around 20 %. The goal of this thesis was the improvement of this system in terms of higher yields and the extension of the product scope to produce resveratrol **6** and pterostilbene **8**.

The chemo-enzymatic tandem setup used in this thesis to produce hydroxystilbene **4**, resveratrol **6** and pterostilbene **8** consisted of two major parts. The first part was an enzymatic decarboxylation to convert coumaric acid **1** to vinylphenol **2** using *BsPAD* encapsulated in alginate beads. While this step worked with full conversion and quantitative yield, the second step of palladium catalyzed Heck coupling required considerable optimization.

To evaluate which parameters influence yield and byproduct formation in the Heck coupling reaction, the optimum process conditions were investigated in several batch experiments. Due to temperature limitations in batch mode, only hydroxystilbene **4** could be synthesized in batch experiments and was consequently used as model substance for all the other products.

While solvent composition and molar equivalents of the substrates were already optimized in a previous work by Kristian Gavric⁴, variation of pH-value and carbonate concentration were promising to further improve the reaction yield. These two parameters were varied independently between 0-100 mM K_2CO_3 and pH-value 10.5-13 along with vinylphenol **2** concentrations between 10-40 mM. First, the basicity and therefore the pH-value was investigated, and all batch experiments showed the same trend regarding yield with an optimum pH range between 11.5-12. Also, the parameter DP/SP was shown not to be influenced by the vinylphenol **2** concentration. Beyond this optimum pH-value window, the yield and DP/SP ratio decreased fast. Afterwards, the K_2CO_3 concentration was varied while the pH-value was kept constant at 11.75. Less byproduct **4b** was formed at higher carbonate concentrations, which led to increasing DP/SP ratios. Unfortunately, the opposite trend was revealed for the yield and as the predominant goal of this thesis was to increase it, a low concentration of 15 mM K_2CO_3 was used for the following experiments. With the new optimized process conditions (pH 11.75, 15 mM K_2CO_3), a maximum yield of 22.1 % was obtained. These parameters are not connected to the amount of substrate in the tested range and therefore absolute values instead of molar equivalents. Compared to conditions used in the previous work (1.5 mol eq. K_2CO_3 and 10 mM **2**), the yield obtained in batch experiments could be increased by 38 %.⁴

After the batch optimization, the Heck coupling reaction was optimized in continuous flow focusing on the reaction temperature as parameter of interest. All desired products were synthesized in continuous flow at temperatures between 80-200 °C. In all experiments a higher

yield with increasing temperature could be observed. However, the higher the temperature, the faster the catalyst degradation and consequently more homocoupling product formed. A good comparison between the products can be made using the average yield within 60 minutes summarized in Table 10. The best yield (49.7 %) could be achieved for hydroxystilbene **4** followed by pterostilbene **8** (48.2 %). Compared to the previous work of Gavric⁴ and Grabner³, the yield of hydroxystilbene **4** could be more than doubled. For resveratrol **6** only 21.9 % average yield could be achieved, which could be possibly explained by the polar hydroxy groups that substantially changed the electronic effects for the coupling reaction as well as the solubility behavior. Furthermore, the real temperature optimum could not be found as catalyst degradation occurred at high temperatures. Experiments starting already at high temperatures and changing the catalyst bed at every temperature stage could be done to overcome this problem. Due to the considerable catalyst leaching at high temperatures, a compromise between high yield and catalyst stability had to be made for the chemo-enzymatic tandem to ensure a stable process for more than 300 minutes.

Table 10 Best experimental results, **4** hydroxystilbene, **6** resveratrol, **8** pterostilbene

	Heck Flow Experiments			Tandem Flow Experiments		
	4	6	8	4	6	8
Maximum Yield [%]	70.5	24.5	50.2	56.9	32.7	62.3
Time Average Yield [%] ¹	49.7	21.9	48.2	54.5	32.1	50.1
Time Average Conversion(2) [%] ¹	100	96.3	78.3	85.0	93.18	76.7
Time Average DP/HP ^{1,2}	4.30	8.85 ³	6.38	7.36	5.75 ³	3.19
Max. Prod. Concentration [mM]	7.05	2.44	5.02	5.39	3.10	5.90

¹Time average values over minimum 60 minutes

²Ratio between desired product and homocoupling product [mM/mM]

³HPLC areas used

In the tandem setup, the decarboxylation of coumaric acid **1** worked with full conversion and quantitative yield. The bottleneck of the system was the Heck coupling step, which worked best for the synthesis of hydroxystilbene **4** with 54.5 % overall average yield over a period of 60 minutes. A similar average yield could be achieved for pterostilbene **8** with 50.1 %. The worst results were obtained for resveratrol **6** with only 32.7 % yield, however, highest conversion of vinylphenol **2** was observed for this product. Least homoproduct was formed in the synthesis of hydroxystilbene **4** with an DP/HP of 7.4 followed by the resveratrol **6** synthesis with 5.8 and pterostilbene **8** synthesis with 3.2.

In general, better results in terms of product formation could be observed for the tandem setup compared to the Heck coupling in flow alone. The CO₂ released during the decarboxylation dissolved in the solvent and had an influence on the basicity and the carbonate concentration.

This effect was not tested in batch experiments and might change the set pH. To evaluate this impact and keep the amount of test runs low, the pH-value of the outlet flow could be measured periodically and correlated to the basicity of the system to further optimize the system towards higher yields. Furthermore, the impact of higher flow rates could be evaluated and optimized.

In batch experiments, it was demonstrated that higher vinylphenol concentrations improve the reaction yield. Therefore, other reactor types like continuous stirred tank reactors could be used to increase the vinylphenol concentrations as already demonstrated by Grabner and Gavric.^{3,4}

As the solvent mixture used contains more than 33 vol.% of ethanol, the influence of this solvent on extraction processes using ethyl acetate was evaluated. The dimensionless partition coefficient of resveratrol decreased from 82 for ethanol-free solvents to 14 for a solvent mixture containing 33 vol.% ethanol.

As catalyst degradation and leaching played a major role throughout this thesis and limited the process in many perspectives, the concept of “palladium swing catalysis” was introduced. The catch-and-release characteristics of the active species was used to retain it within the reactor zone by changing the flow direction periodically. The feasibility of this concept was proven experimentally. In one experiment, the active species was pushed towards the end of a catalyst bed. Afterwards, the flow direction was inverted and the active species could then be found at the other end of the column, the former front. Another experiment proved that the active species could be captured in a palladium free SCM catalyst bed, which was placed at the front as well at the end of the regular palladium catalyst packed bed. However, to use this concept practically, further experiments need to be performed. The kinetics of the catalyst leaching must be evaluated to identify suitable time intervals for the inversion of flow direction without pushing too much active material out of the system. The catalyst particle size, temperature and flow rate play an important role and their influence needs to be evaluated. Qualitatively, it could already be observed that smaller catalyst particles tend to leach faster but showed an increased activity. Nevertheless, it could be demonstrated that the „palladium swing catalysis” is a promising method to increase the industrial suitability of the heterogenous palladium catalysis. Together with increased yield and the feasible broad product portfolio our synthesis process is a good starting point to develop a related large-scale production for stilbene derivatives.

6 Appendix

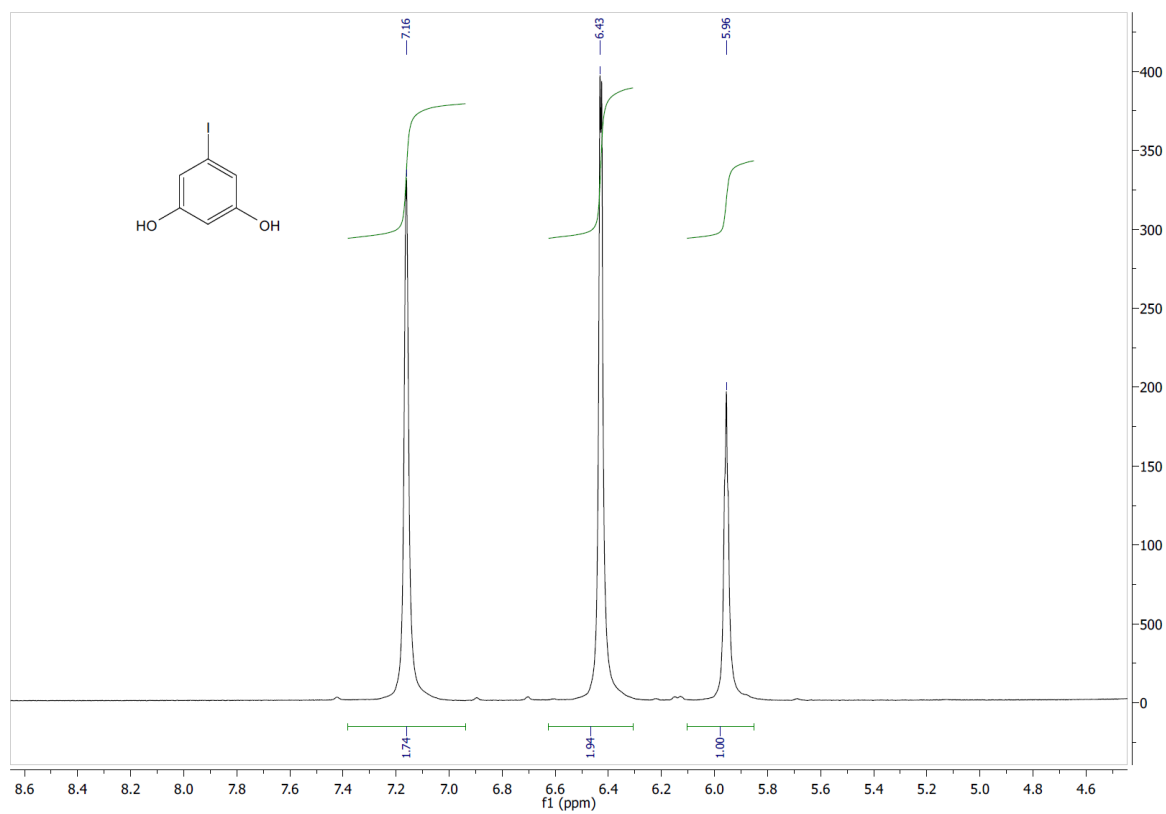


Figure 21 $^1\text{H-NMR}$ (300 MHz, C_6D_6) spectrum of 2,4-dihydroxyiodobenzene **5**

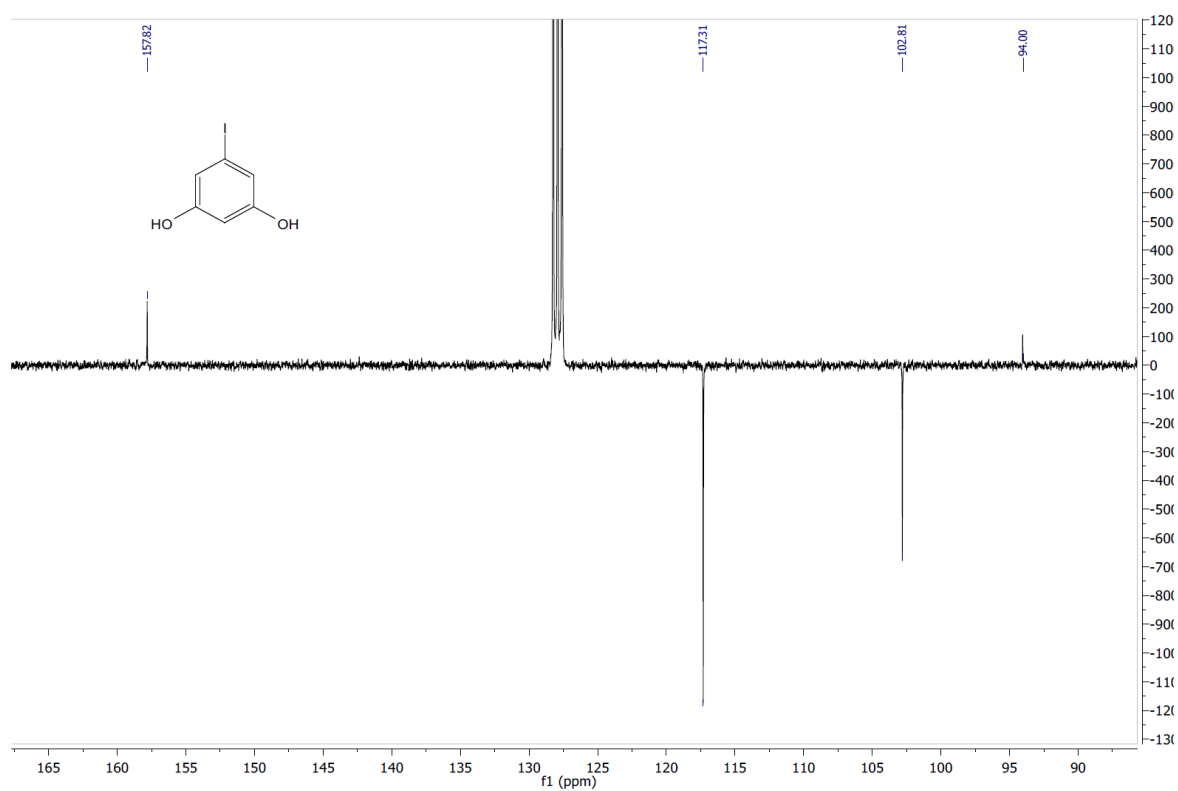


Figure 22 $^{13}\text{C-NMR}$ (76 MHz, APT, C_6D_6) spectrum of 2,4-dihydroxyiodobenzene **5**

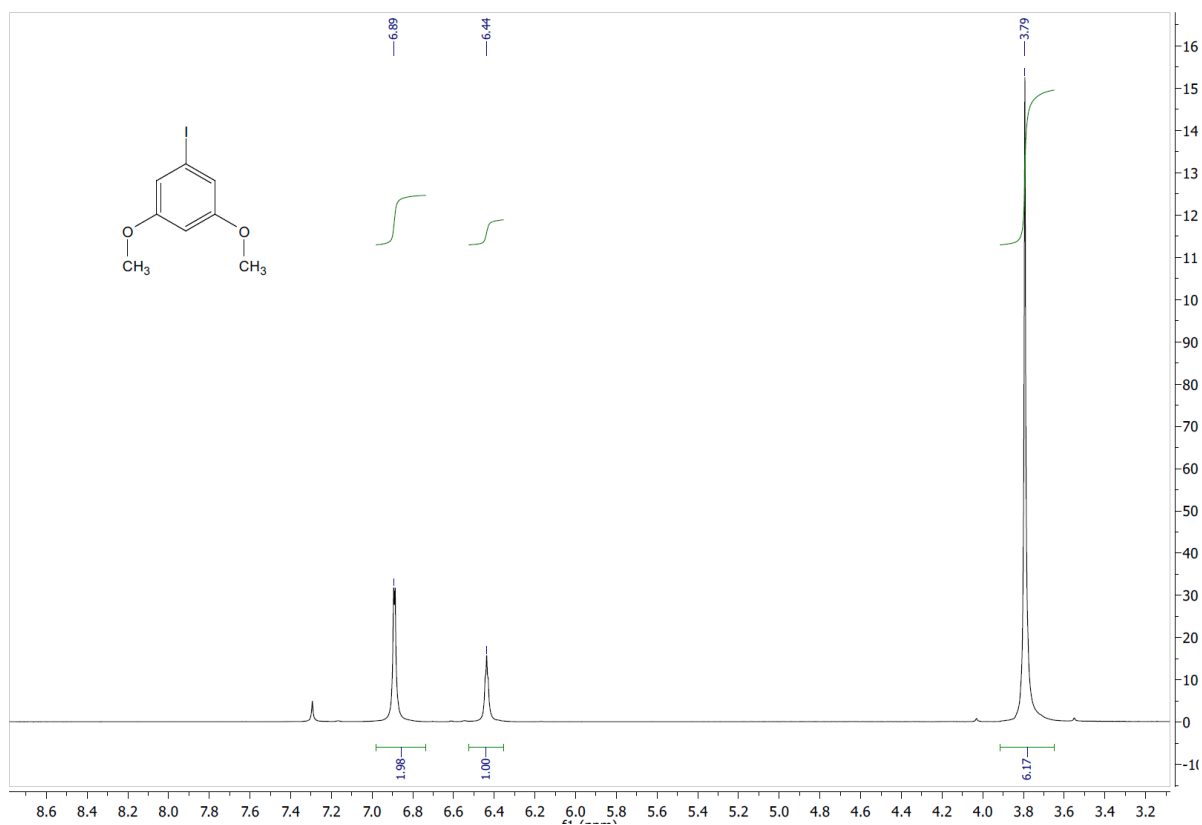


Figure 23 $^1\text{H-NMR}$ (300 MHz, CDCl_3) spectrum of 2,4-dimethoxyiodobenzene **7**

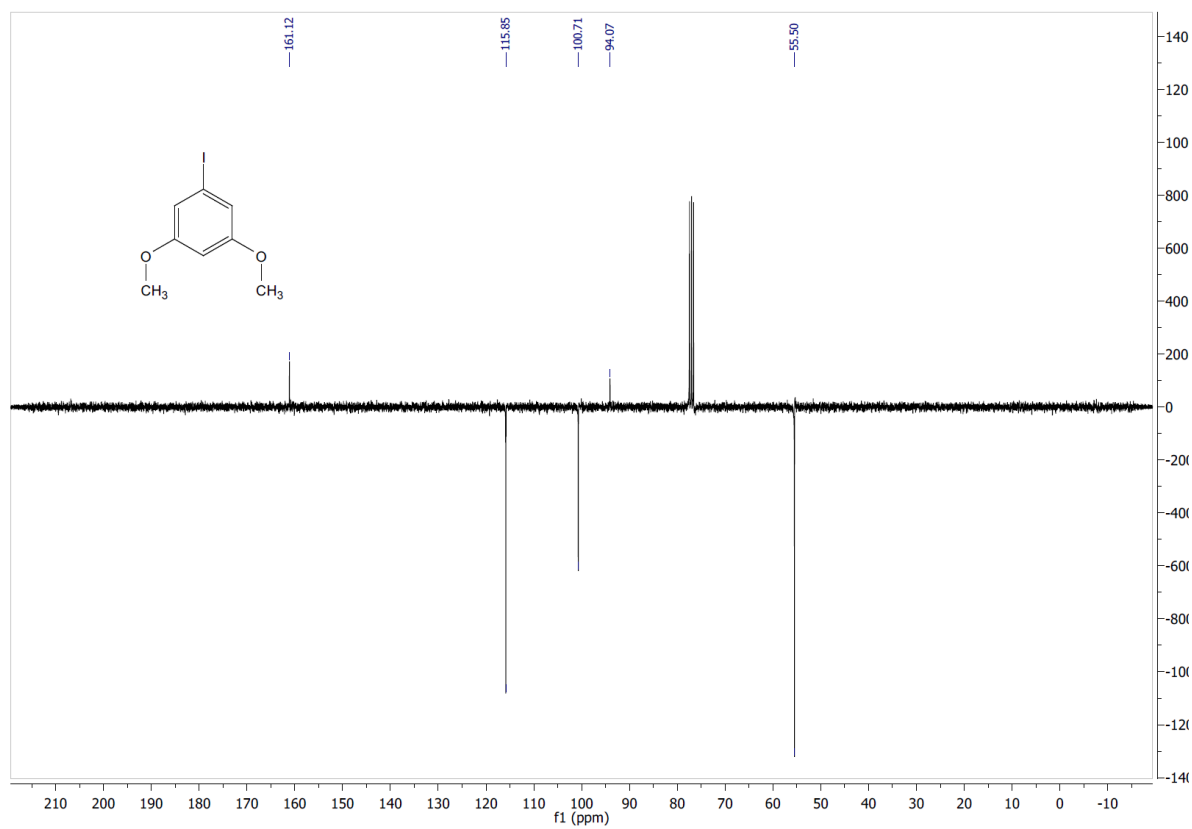


Figure 24 $^{13}\text{C-NMR}$ (76 MHz, APT, CDCl_3) spectrum of 2,4-dimethoxyiodobenzene **7**

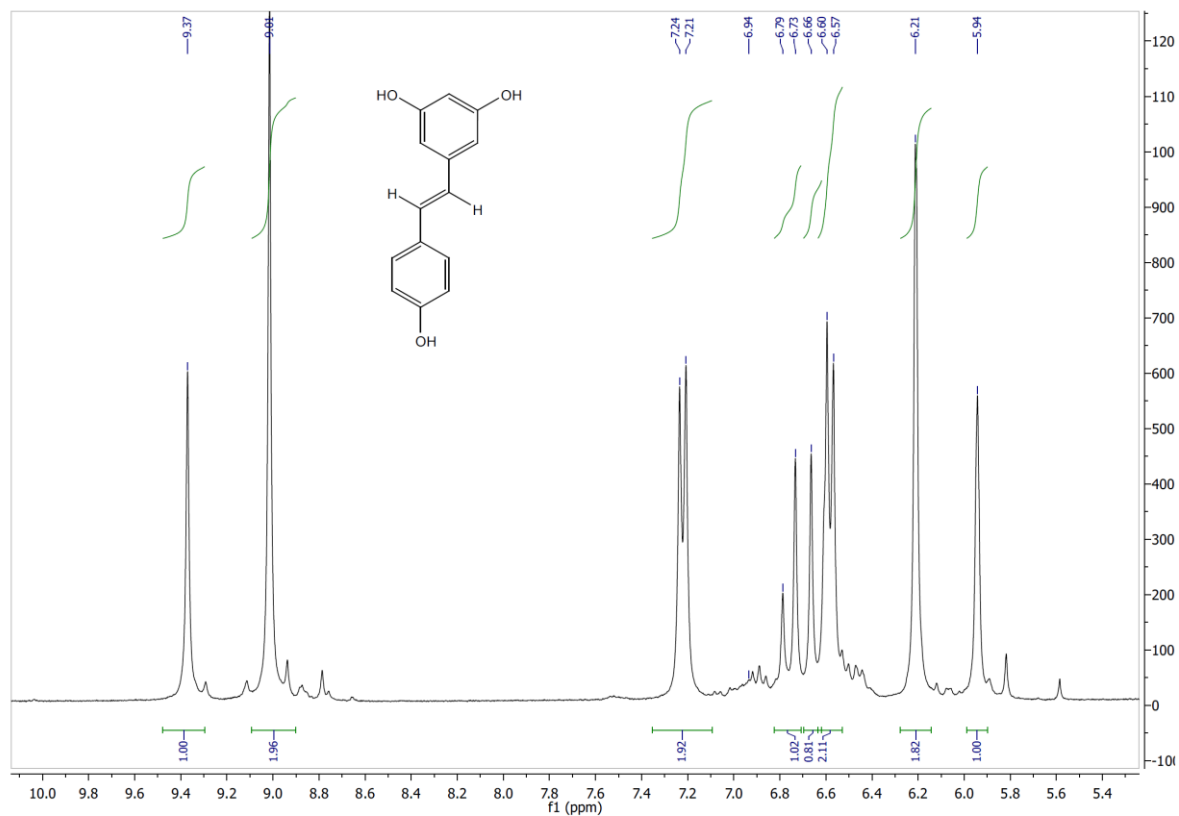


Figure 25 ¹H-NMR (300 MHz, DMSO-d₆) spectrum of resveratrol 6

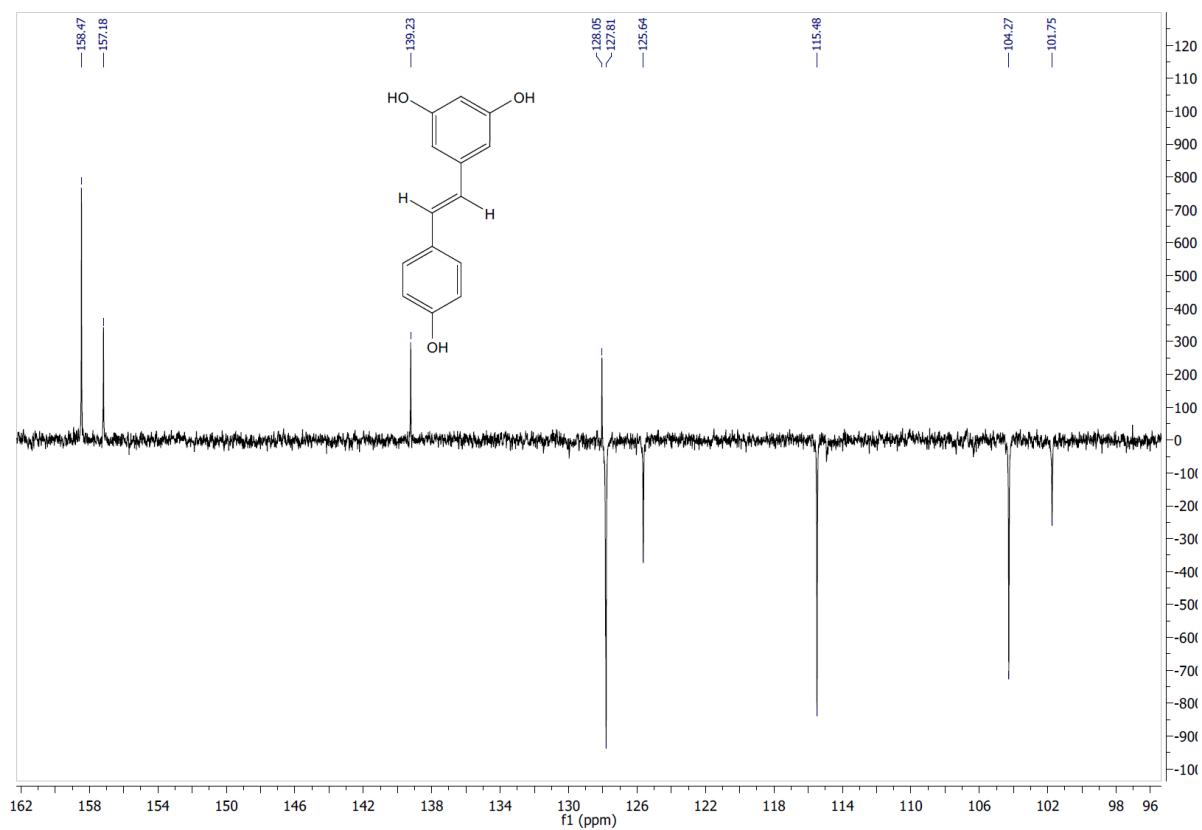


Figure 26 ¹³C-NMR (76 MHz, APT, DMSO-d₆) spectrum of resveratrol 6

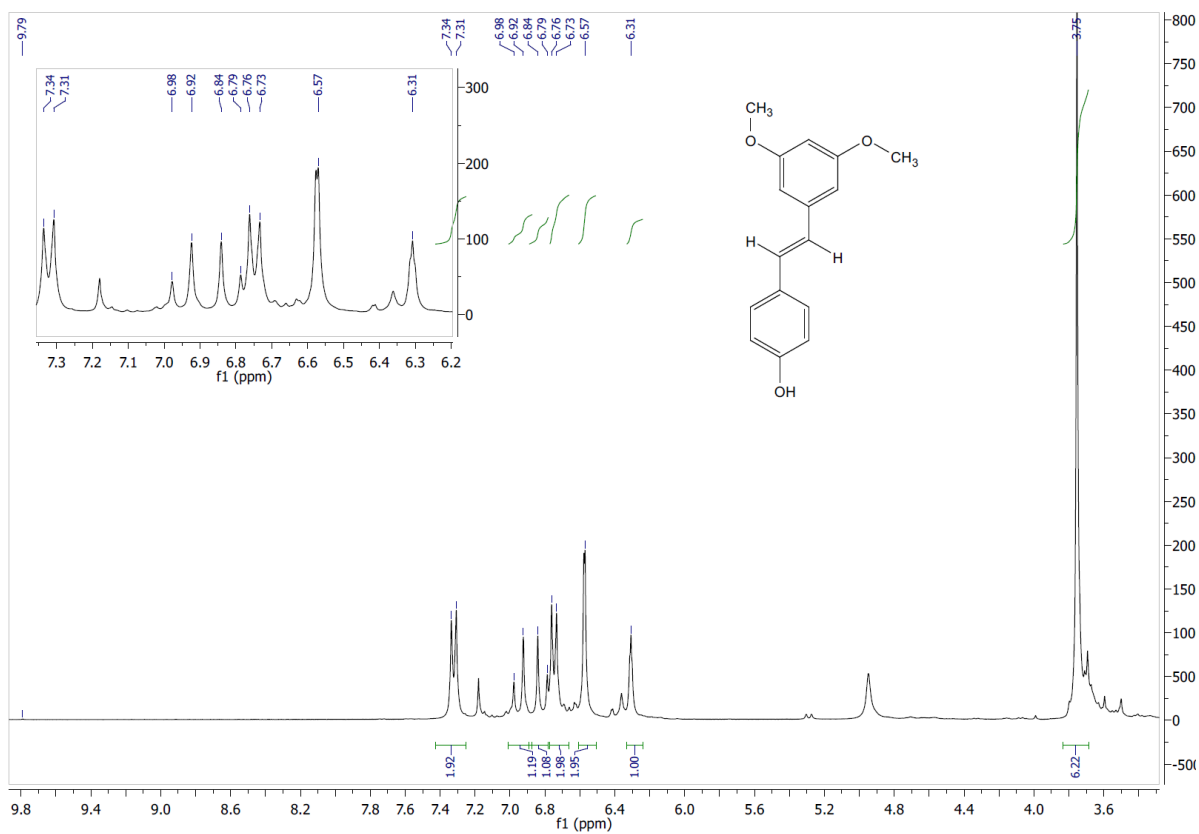


Figure 27 $^1\text{H-NMR}$ (300 MHz, CDCl_3) spectrum of pterostilbene **8**

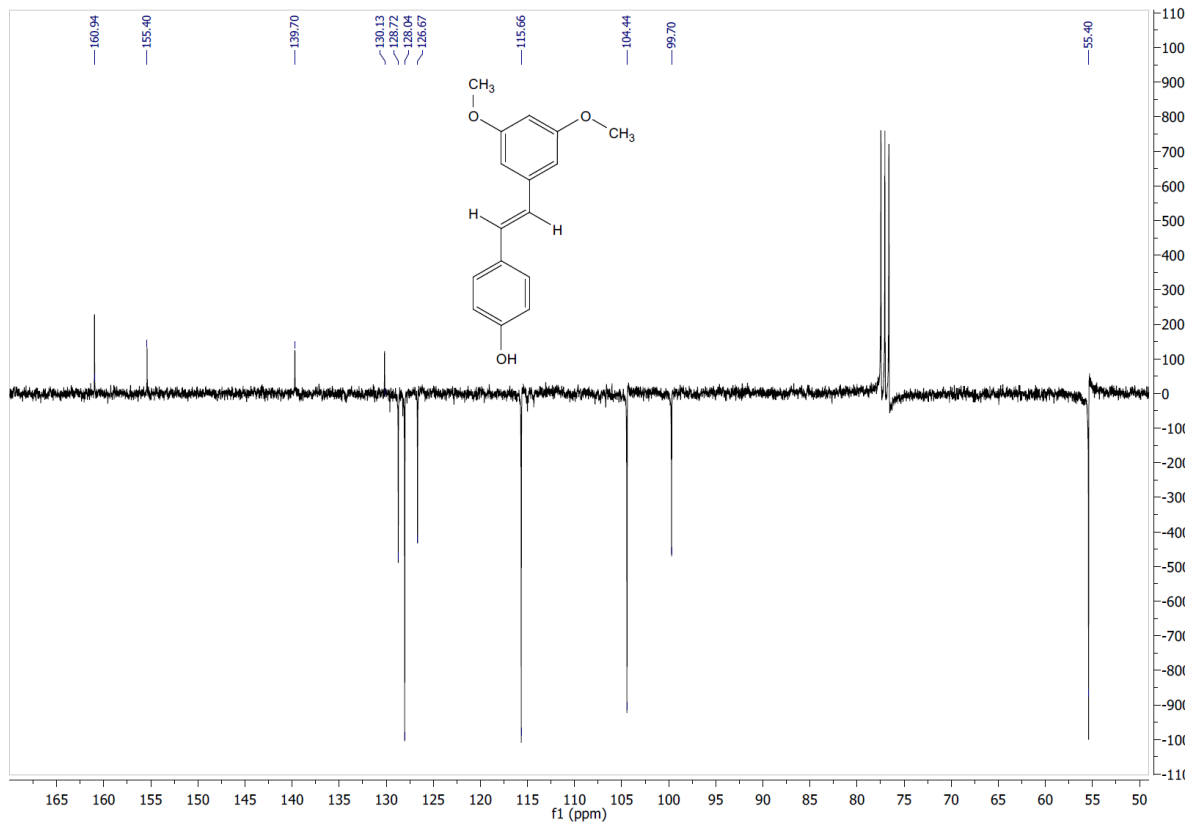


Figure 28 $^{13}\text{C-NMR}$ (76 MHz, APT, CDCl_3) spectrum of pterostilbene **8**

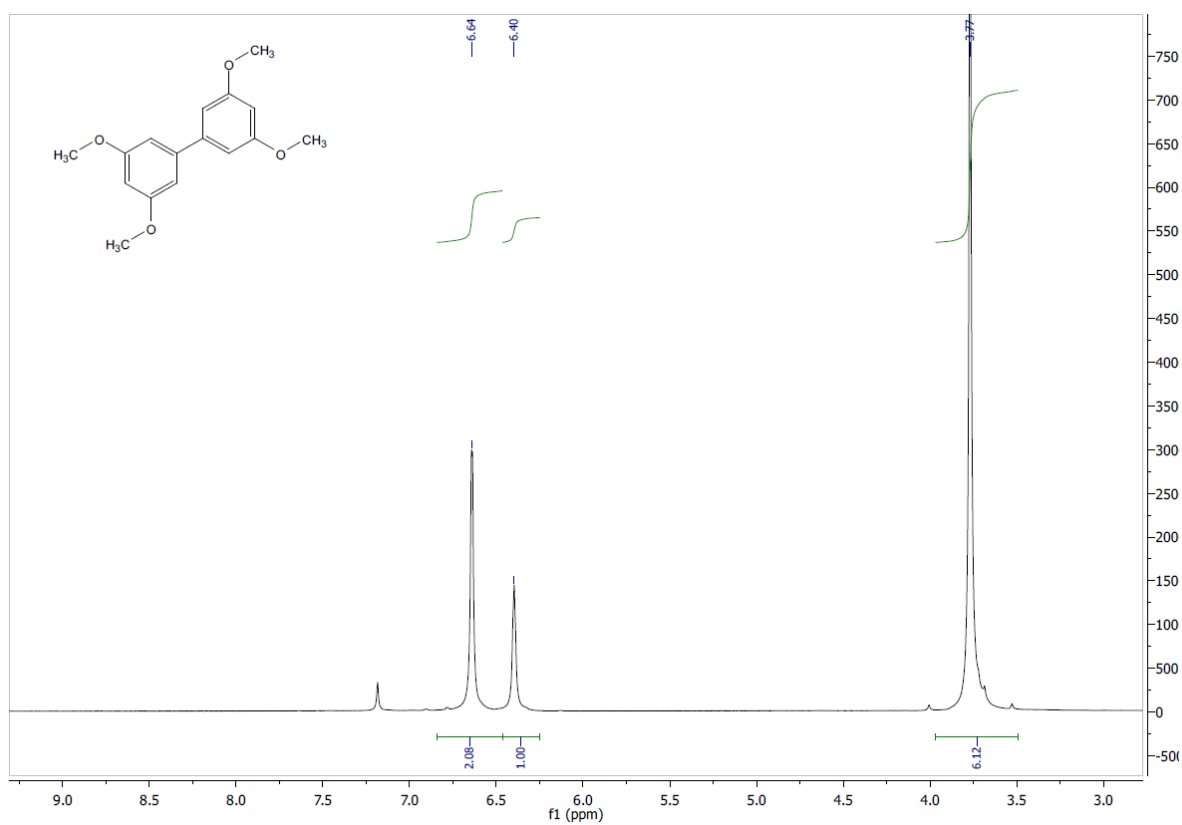


Figure 29 $^1\text{H-NMR}$ (300 MHz, APT, CDCl_3) spectrum of 3,3',5,5'-tetramethoxy-1,1'-biphenyl **8a**

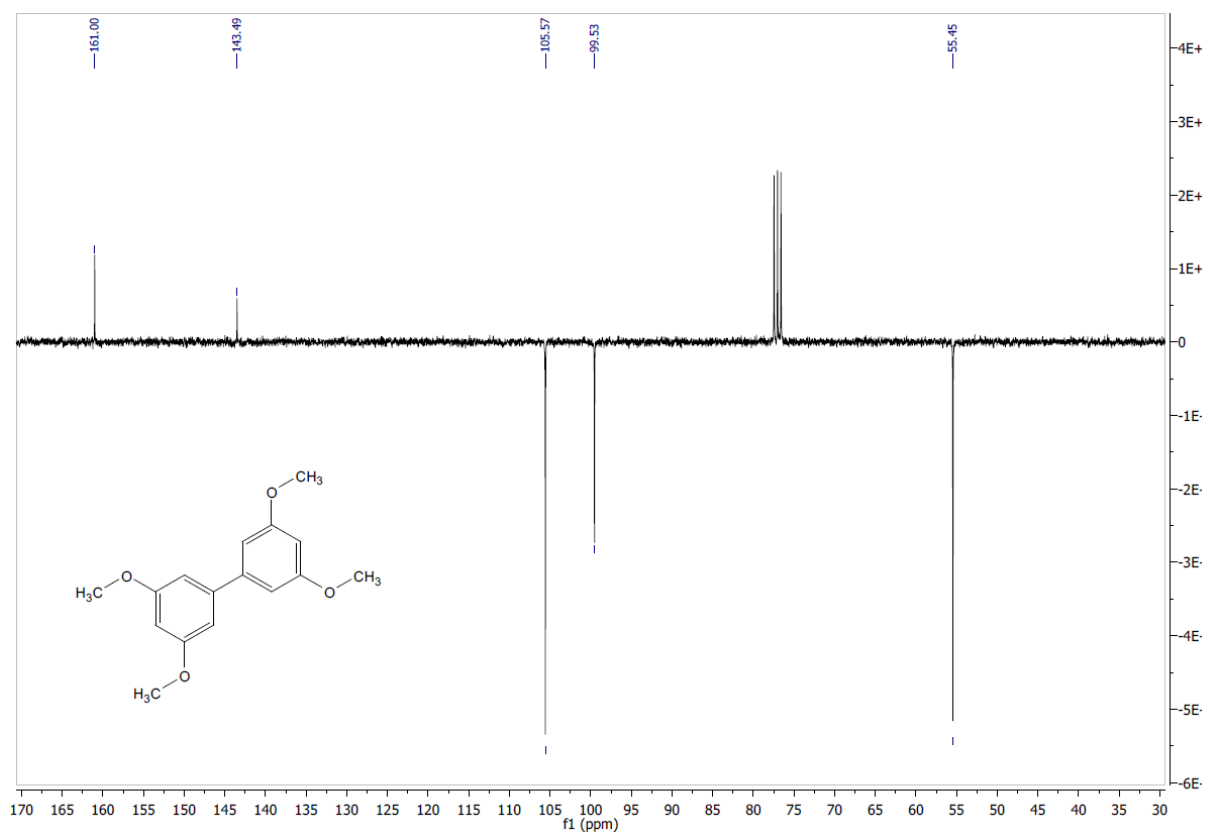


Figure 30 $^{13}\text{C-NMR}$ (76 MHz, APT, CDCl_3) spectrum of 3,3',5,5'-tetramethoxy-1,1'-biphenyl **8a**

7 Abbreviations and Symbol Directory

API	Active pharmaceutical ingredient
ArX	Aryl halide
BPR	Back pressure regulator
BsPAD	Phenolic acid decarboxylase from <i>Bacillus subtilis</i>
CDCl₃	Deuterated chloroform
CFE	Cell-free extract
ChCl	Choline chloride
c_i	Concentration of tracer
CSTR	Continuous stirred tank reactor
C₆D₆	Deuterated benzene
DES	Deep eutectic solvent
DMSO	Dimethylsulfoxide
DP/SP	Desired product/Side product ratio
DP/HP	Desired product/ homocoupling product ratio
ee	Enantiomeric excess
EtOAc	Ethyl acetate
EtOH	Ethanol
HBD	Hydrogen bond donator
HPLC	High performance liquid chromatography
KPi-buffer	Potassium phosphate buffer
MTBE	Methyl <i>tert.</i> butyl ether
PE	Petrol ether

SCM	Solution combustion method
TLC	Thin layer chromatography
t_i	time since signal change
Tol	Toluene
VP	Vinylphenol

8 List of Figures

Figure 1 Structures of important biologically active stilbene derivatives (stilbene core-structure highlighted in red).....	2
Figure 2 Continuous dynamic kinetic resolution to produce enantiopure amides (scheme reproduced from ²²)	6
Figure 3 Catalytic cycles of Heck reaction using a)homogeneous palladium in the presence of a ligand, and b) the concept of “ligandless” palladium catalysis (reproduced from ²⁸)	8
Figure 4 Enzymatic decarboxylation mechanism catalyzed by Lactobacillus phenolic acid decarboxylase (target molecule in blue, reproduced from ³¹)	11
Figure 5 Na-alginate encapsulation with Ca ²⁺ -Ions (reproduced from ³⁵)	13
Figure 6 Surface plot of pH-value and vinylphenol (VP) 2 concentration influencing product yield; batch experiments according to chapter 4.3.5	15
Figure 7 Surface plot of pH-value and vinylphenol (VP) 2 concentration influencing DP 4 /SP 4b peak area ratio; batch experiments according to chapter 4.3.5.....	16
Figure 8 Influence of K ₂ CO ₃ concentration on yield (orange) and DP 4 /SP 4b peak area ratio (blue) with two different vinylphenol 2 concentrations and constant pH of 11.75; batch experiments according to chapter 4.3.5.; for better visualization points are connected	17
Figure 9 Heck reaction in continuous flow for formation of hydroxystilbene 4 ; concentrations of vinylphenol 2 (blue), homocoupling product 4a (grey), hydroxystilbene 4 (orange) and iodobenzene 3 (green) over reaction time; temperature profile (black) on secondary axis; experiment conducted according to chapter 4.4.1 with 10 mM of 2	20
Figure 10 Heck reaction in flow for synthesis of resveratrol 6 ; concentrations of vinylphenol 2 (blue), homocoupling product 6a (grey) and resveratrol 6 (orange) over reaction time; temperature profile (black) on secondary axis; experiment conducted according to chapter 4.4.1 with 10 mM of 2	21
Figure 11 Heck reaction in flow for synthesis of pterostilbene 8 ; concentrations of vinylphenol 2 (blue), homocoupling product 8a (grey), pterostilbene 8 (orange) and 2,4-dimethoxyiodobenzene 7 (green) over reaction time; temperature profile (black) on secondary axis; experiment conducted according to chapter 4.4.1 with 10 mM of 2	22
Figure 12 Tandem flow experiment results; conversion (blue), yield (orange), desired product 4 to homocoupling product 4a peak area ratio (grey, sec. axis) and), desired product 4 to side product 4b peak area ratio (yellow, sec. axis); experiments conducted according to chapter 4.4.2	25

Figure 13 Tandem flow experiment results; conversion (blue), yield (orange), desired product 6 to homocoupling product 6a peak area ratio (grey, sec. axis); experiments conducted according to chapter 4.4.2	26
Figure 14 Tandem flow experiment results; conversion (blue), yield (orange), desired product 8 to homocoupling product 8a peak area ratio (grey, sec. axis); experiments conducted according to chapter 4.4.2	27
Figure 15 Partition coefficient of resveratrol; aqueous phase: solvent mixture [DES (30 %):KPI (25 %):H ₂ O (45-φ%):EtOH (φ %)] (vol.%; organic phase: ethyl acetate; 1:1 (v/v) mixture single stage in equilibrium	28
Figure 16 Concept of "Palladium Swing Catalysis", First row shows active species concentration profile for the Pd-swing catalysis: 1 t = 0 starting point , 2 t = t _{1/2} half of the active species is pushed out of the Pd-section(t _{1/2})-change of flow direction, 3 t = 2 t _{1/2} the active species is pushed to the former front section of the Pd-section - the total system is still catalytically active; Second row shows regular case: 1 t = 0 starting point, 2 t = t _{1/2} half of the active species is pushed out of the system, 3 t = 2 t _{1/2} all of the active species is pushed out of the system-system in not catalytically active anymore	30
Figure 17 Activity, conversion (2) and yield (4) of different column positions in a palladium swing catalysis setup without recovery sections, flow direction change after 120 minutes, according to procedure 4.4.4	32
Figure 18 Activity, conversion (2) , yield (4) of different column positions, Pd-column followed by a recovery column without change of flow direction, both columns washed with 10 times the column volume	33
Figure 19 Multiple batch setup for Heck couplings (in the heat up phase)	35
Figure 20 Chemo enzymatic tandem setup	43
Figure 21 ¹ H-NMR (300 MHz, C ₆ D ₆) spectrum of 2,4-dihydroxy iodobenzene 5	49
Figure 22 ¹³ C-NMR (76 MHz, APT, C ₆ D ₆) spectrum of 2,4-dihydroxyiodobenzene 5	49
Figure 23 ¹ H-NMR (300 MHz, CDCl ₃) spectrum of 2,4-dimethoxyiodobenzene 7	50
Figure 24 ¹³ C-NMR (76 MHz, APT, CDCl ₃) spectrum of 2,4-dihydroxyiodobenzene 7	50
Figure 25 ¹ H-NMR (300 MHz, DMSO-d ₆) spectrum of resveratrol 6	51
Figure 26 ¹³ C-NMR (76 MHz, APT, DMSO-d ₆) spectrum of resveratrol 6	51
Figure 27 ¹ H-NMR (300 MHz, CDCl ₃) spectrum of pterostilbene 8	52
Figure 28 ¹³ C-NMR (76 MHz, APT, CDCl ₃) spectrum of pterostilbene 8	52
Figure 29 ¹ H-NMR (300 MHz, APT, CDCl ₃) spectrum of 3,3',5,5'-tetramethoxy-1,1'-biphenyl 8a	53
Figure 30 ¹³ C-NMR (76 MHz, APT, CDCl ₃) spectrum of 3,3',5,5'-tetramethoxy-1,1'-biphenyl 8a	53

9 List of Schemes

Scheme 1 Heck coupling experiments in batch using standard batch conditions according to chapter 4.3.5; substrates: vinylphenol 2 , iodobenzene 3 ; products: hydroxystilbene 4 , biphenyl 4a , para-hydroxy-1,1-diphenylethylene 4b ; catalyst produced with solution combustion method (SCM).....	14
Scheme 2 Continuous Heck coupling experiments; different substrates and process conditions were used according to Table 2 and Table 3; flow experiments conducted according to chapter 4.4.1.; base was added to substrate mixture	18
Scheme 3 Tandem flow experiment comprising enzymatic decarboxylation as well as Heck coupling of vinylphenol with various iodoaryl substrate to give stilbenes; ; first syringe pump(left) provides a 20 mM coumaric acid 1 solution in DES:KPi 1:1 for the decarboxylation column filled with 160 mg BsPAD immobilized in enzyme beads; the product vinylphenol 2 is coupled with various iodoaryl substrates 3 , 5 and 7 dissolved in DES:EtOH:H ₂ O 1:6.75:2.25 plus base entering the system through another syringe pump (middle); Heck coupling is performed in a packed bed reactor with Pd-SCM catalyst at 145 °C and 0.2 mL/min flowrate	24
Scheme 4 Synthesis of 5-iodobenzene-1,3-diol 5 , procedure from ³⁹	39
Scheme 5 Synthesis of 3,5-dimethoxy-1-iodobenzene 7 , procedure from ⁴⁰	40

10 List of Tables

Table 1 Maximum acceptable concentrations limits for residues of metal catalysts for pharmaceuticals ²⁷	7
Table 2 Substrates, products and homocoupling side products used and synthesized in continuous Heck coupling experiments	18
Table 3 Experimental parameters and analyzed parameters of continuous Heck coupling reactions according to chapter 4.4.1	19
Table 4 HPLC methods, methanol and buffer (H ₂ O:H ₃ PO ₄ 300:1) gradients.....	36
Table 5 Retention time and detector wavelength for analyzed compounds.....	36
Table 6 List of: Substrates and K ₂ CO ₃ concentrations as well as different pH-values used for batch Heck couplings	38
Table 7 Experiment parameters and analyzed parameters of continuous Heck coupling reactions.....	41
Table 8 Pump setup for residence time distribution measurements.....	44
Table 9 Results residence time distribution measurements	44
Table 10 Best experimental results, 4 hydroxystilbene, 6 resveratrol, 8 pterostilbene	47

11 Bibliography

1. Tsai, H. Y.; Ho, C. T.; Chen, Y. K., Biological actions and molecular effects of resveratrol, pterostilbene, and 3'-hydroxypterostilbene. *J Food Drug Anal* **2017**, *25* (1), 134-147.
2. Kiselev, K. V., Perspectives for production and application of resveratrol. *Appl Microbiol Biotechnol* **2011**, *90* (2), 417-25.
3. Grabner, B.; Schweiger, A. K.; Gavric, K.; Kourist, R.; Gruber-Woelfler, H., A chemo-enzymatic tandem reaction in a mixture of deep eutectic solvent and water in continuous flow. *Reaction Chemistry & Engineering* **2020**, *5* (2), 263-269.
4. Gavric, K., Development of a Continuous Chemo-Enzymatic Two-Step Synthesis of Resveratrol Derivatives. *TU Graz Master Thesis* **2020**.
5. Chemie, R. L. Eintrag zu Stilben [https://roempp.thieme.de/lexicon/RD-19-04149\(09/2020\)](https://roempp.thieme.de/lexicon/RD-19-04149(09/2020)).
6. Kwasniewski, S. P.; Claes, L.; François, J.-P.; Deleuze, M. S., High level theoretical study of the structure and rotational barriers of trans-stilbene. *The Journal of Chemical Physics* **2003**, *118* (17), 7823-7836.
7. Lamuela-Raventos, R. M.; Romero-Perez, A. I.; Waterhouse, A. L.; de la Torre-Boronat, M. C., Direct HPLC Analysis of cis- and trans-Resveratrol and Piceid Isomers in Spanish Red *Vitis vinifera* Wines. *Journal of Agricultural and Food Chemistry* **1995**, *43* (2), 281-283.
8. Prokop, J.; Abrman, P.; Seligson, A. L.; Sovak, M., Resveratrol and its glycon piceid are stable polyphenols. *J Med Food* **2006**, *9* (1), 11-4.
9. Takaoka, M., The Phenolic Substances of White Hellebore (*Veratrum Grandiflorum* Hoes. Fil.) I. *Nippon Kagaku Kaishi* **1939**, *60* (11), 1090-1100.
10. Coussens, L. M.; Werb, Z., Inflammation and cancer. *Nature* **2002**, *420* (6917), 860-867.
11. Cui, X.; Jin, Y.; Hofseth, A. B.; Pena, E.; Habiger, J.; Chumanevich, A.; Poudyal, D.; Nagarkatti, M.; Nagarkatti, P. S.; Singh, U. P.; Hofseth, L. J., Resveratrol Suppresses Colitis and Colon Cancer Associated with Colitis. *Cancer Prevention Research* **2010**, *3* (4), 549-559.
12. Lee, J. A.; Ha, S. K.; Cho, E.; Choi, I., Resveratrol as a Bioenhancer to Improve Anti-Inflammatory Activities of Apigenin. *Nutrients* **2015**, *7* (11), 9650-61.
13. Chang, C.-W.; Chen, Y.-M.; Hsu, Y.-J.; Huang, C.-C.; Wu, Y.-T.; Hsu, M.-C., Protective effects of the roots of *Angelica sinensis* on strenuous exercise-induced sports anemia in rats. *Journal of Ethnopharmacology* **2016**, *193*, 169-178.
14. Gutmann, B.; Cantillo, D.; Kappe, C. O., Continuous-flow technology—a tool for the safe manufacturing of active pharmaceutical ingredients. *Angew Chem Int Ed Engl* **2015**, *54* (23), 6688-728.
15. Wirth, T., Microreactors in organic chemistry and catalysis. **2013**.
16. Curzons, A. D.; Constable, D. J. C.; Mortimer, D. N.; Cunningham, V. L., So you think your process is green, how do you know?—Using principles of sustainability to determine what is green—a corporate perspective. *Green Chemistry* **2001**, *3* (1), 1-6.
17. Gutmann, B.; Kappe, C. O., Forbidden chemistries — paths to a sustainable future engaging continuous processing. *Journal of Flow Chemistry* **2017**, *7* (3–4), 65-71.

18. Yoshida, J. i., Introduction. *Flash Chemistry* **2008**, 1-5.
19. Jähnisch, K.; Hessel, V.; Löwe, H.; Baerns, M., Chemie in Mikrostrukturreaktoren. *Angewandte Chemie* **2004**, *116* (4), 410-451.
20. Sperl, J. M.; Carsten, J. M.; Guterl, J.-K.; Lommes, P.; Sieber, V., Reaction Design for the Compartmented Combination of Heterogeneous and Enzyme Catalysis. *ACS Catalysis* **2016**, *6* (10), 6329-6334.
21. Peng, M.; Mittmann, E.; Wenger, L.; Hubbuch, J.; Engqvist, M. K. M.; Niemeyer, C. M.; Rabe, K. S., 3D-Printed Phenacrylate Decarboxylase Flow Reactors for the Chemoenzymatic Synthesis of 4-Hydroxystilbene. *Chemistry* **2019**.
22. Farkas, E.; Olah, M.; Foldi, A.; Koti, J.; Eles, J.; Nagy, J.; Gal, C. A.; Paizs, C.; Hornyanszky, G.; Poppe, L., Chemoenzymatic Dynamic Kinetic Resolution of Amines in Fully Continuous-Flow Mode. *Org Lett* **2018**, *20* (24), 8052-8056.
23. Heck, R. F.; Nolley, J. P., Palladium-catalyzed vinylic hydrogen substitution reactions with aryl, benzyl, and styryl halides. *The Journal of Organic Chemistry* **1972**, *37* (14), 2320-2322.
24. Johansson Seechurn, C. C.; Kitching, M. O.; Colacot, T. J.; Snieckus, V., Palladium-catalyzed cross-coupling: a historical contextual perspective to the 2010 Nobel Prize. *Angew Chem Int Ed Engl* **2012**, *51* (21), 5062-85.
25. Jagtap, S., Heck Reaction—State of the Art. *Catalysts* **2017**, *7* (9).
26. Christoffel, F.; Ward, T. R., Palladium-Catalyzed Heck Cross-Coupling Reactions in Water: A Comprehensive Review. *Catalysis Letters* **2017**, *148* (2), 489-511.
27. Mpungose, P. P.; Vundla, Z. P.; Maguire, G. E. M.; Friedrich, H. B., The Current Status of Heterogeneous Palladium Catalysed Heck and Suzuki Cross-Coupling Reactions. *Molecules* **2018**, *23* (7).
28. Cantillo, D.; Kappe, C. O., Immobilized Transition Metals as Catalysts for Cross-Couplings in Continuous Flow-A Critical Assessment of the Reaction Mechanism and Metal Leaching. *ChemCatChem* **2014**, *6* (12), 3286-3305.
29. Lichtenegger, G. J.; Maier, M.; Hackl, M.; Khinast, J. G.; Gössler, W.; Griesser, T.; Kumar, V. S. P.; Gruber-Woelfler, H.; Deshpande, P. A., Suzuki-Miyaura coupling reactions using novel metal oxide supported ionic palladium catalysts. *Journal of Molecular Catalysis A: Chemical* **2017**, *426*, 39-51.
30. Landete, J. M.; Rodriguez, H.; Curiel, J. A.; de las Rivas, B.; Mancheno, J. M.; Munoz, R., Gene cloning, expression, and characterization of phenolic acid decarboxylase from *Lactobacillus brevis* RM84. *J Ind Microbiol Biotechnol* **2010**, *37* (6), 617-24.
31. Rodriguez, H.; Angulo, I.; de Las Rivas, B.; Campillo, N.; Paez, J. A.; Munoz, R.; Mancheno, J. M., p-Coumaric acid decarboxylase from *Lactobacillus plantarum*: structural insights into the active site and decarboxylation catalytic mechanism. *Proteins* **2010**, *78* (7), 1662-76.
32. Gomez Baraibar, A.; Reichert, D.; Mugge, C.; Seger, S.; Groger, H.; Kourist, R., A One-Pot Cascade Reaction Combining an Encapsulated Decarboxylase with a Metathesis Catalyst for the Synthesis of Bio-Based Antioxidants. *Angew Chem Int Ed Engl* **2016**, *55* (47), 14823-14827.
33. Mohamad, N. R.; Marzuki, N. H.; Buang, N. A.; Huyop, F.; Wahab, R. A., An overview of technologies for immobilization of enzymes and surface analysis techniques for immobilized enzymes. *Biotechnol Biotechnol Equip* **2015**, *29* (2), 205-220.
34. Trelles, J. A.; Rivero, C. W., Whole Cell Entrapment Techniques. In *Immobilization of Enzymes and Cells: Third Edition*, Guisan, J. M., Ed. Humana Press: Totowa, NJ, 2013; pp 365-374.

35. Martau, G. A.; Mihai, M.; Vodnar, D. C., The Use of Chitosan, Alginate, and Pectin in the Biomedical and Food Sector-Biocompatibility, Bioadhesiveness, and Biodegradability. *Polymers (Basel)* **2019**, *11* (11).
36. Brazier, J. B.; Nguyen, B. N.; Adrio, L. A.; Barreiro, E. M.; Leong, W. P.; Newton, M. A.; Figueroa, S. J. A.; Hellgardt, K.; Hii, K. K. M., Catalysis in flow: Operando study of Pd catalyst speciation and leaching. *Catalysis Today* **2014**, *229*, 95-103.
37. Bourouina, A.; Meille, V.; de Bellefon, C., A flow split test to discriminating between heterogeneous and homogeneous contributions in Suzuki coupling. *Journal of Flow Chemistry* **2018**, *8* (3-4), 117-121.
38. Baidya, T.; Gupta, A.; Deshpandey, P. A.; Madras, G.; Hegde, M. S., High Oxygen Storage Capacity and High Rates of CO Oxidation and NO Reduction Catalytic Properties of $Ce_{1-x}Sn_xO_2$ and $Ce_{0.78}Sn_{0.2}Pd_{0.02}O_{2-\delta}$. *The Journal of Physical Chemistry C* **2009**, *113* (10), 4059-4068.
39. Müller, J. I.; Kusserow, K.; Hertrampf, G.; Pavic, A.; Nikodinovic-Runic, J.; Gulder, T. A. M., Synthesis and initial biological evaluation of myxocoumarin B. *Organic & Biomolecular Chemistry* **2019**, *17* (7), 1966-1969.
40. Csuk, R.; Albert, S., A Short Synthesis of Rhaponticin and its 3"-Fluoroanalog via a Wittig/Heck-Mizoroki Route. *Zeitschrift für Naturforschung B* **2011**, *66* (3), 311.